Appendix 2.8 A

Task 2.8 A: Investigation of Scale-Up Issues Associated with Ultraviolet Light Disinfection and Reverse Osmosis Desalination

Submitted by:

Alexander A. Mofidi, Christopher J. Gabelich, Tae I. Yun,
Bradley M. Coffey, and James F. Green

Metropolitan Water District of Southern California
La Verne, California

Submitted to:

California Energy Commission
Sacramento, California

January 2002

LEGAL NOTICE

This report was prepared as a result of work sponsored by the California Energy Commission (Commission). It does not necessarily represent the views of the Commission, its employees, or the State of California. The Commission, the State of California, its employees, contractors, and subcontractors make no warranty, express or implied, and assume no legal liability for the information in this report; nor does any party represent that the use of this information will not infringe upon privately owned rights. This report has not been approved or disapproved by the Commission nor has the Commission passed upon the accuracy or adequacy of this information in this report.

ACKNOWLEDGMENTS

Funding for this project was graciously provided by the California Energy Commission's Public Interest Energy Research Program. The authors wish to express their appreciation for the project management by Lory E. Larson, Southern California Edison. Technical and moral support were provided by Bradley M. Coffey, Metropolitan Water District of Southern California, La Verne, California.

The authors are also indebted to Connie Chou, Milton Cox, Hoang Do, Himansu Mehta and Jerry Pitts for their support throughout this project and student interns Erica Wolski and Monique Valenzuela, who conducted the routine sampling and database management for this study. Without their tireless efforts, this project would not have been a success. Additional thanks are extended to the entire Water Quality Laboratory staff at Metropolitan who set up and maintained the research platforms, and collected the data used during this study.

TABLE OF CONTENTS

LIST OF TABLES

LIST OF FIGURES

PREFACE

The Public Interest Energy Research (PIER) Program supports public interest energy research and development that will help improve the quality of life in California by bringing environmentally safe, affordable, and reliable energy services and products to the marketplace.

The PIER Program, managed by the California Energy Commission (Commission), annually awards up to $62 mgdto conduct the most promising public interest energy research by partnering with Research, Development, and Demonstration (RD&D) organizations, including individuals, businesses, utilities, and public or private research institutions.

PIER funding efforts are focused on the following six RD&D program areas:

- Buildings End-Use Energy Efficiency
- Industrial/Agricultural/Water End-Use Energy efficiency
- Renewable Energy
- Environmentally-Preferred Advanced Generation
- Energy-Related Environmental Research
- Strategic Energy Research

What follows is the final report for *Electrotechnology Applications for Potable Water Production and Protection of the Environment,* Contract No. 500-97-044**,** conducted by the Metropolitan Water District of Southern California. The report is entitled "Electrotechnology Applications for Potable Water Production and Protection of the Environment: Task 8 Investigation of Scale-Up Issues Associated with Ultraviolet Light Disinfection and Reverse Osmosis Desalination." This project contributes to the Industrial/Agricultural/Water End-Use Energy Efficiency area.

For more information on the PIER Program, please visit the Commission's Web site at: http://www.energy.ca.gov/research/index/html or contact the Commission's Publications Unit at 916-654-5200.

EXECUTIVE SUMMARY

Drinking water utilities in California are charged with providing both safe and aesthetically pleasing water to their consumers. Increased demands on disinfection requirements, as well as salinity removal, have created new challenges in meeting these goals. This project evaluated the placement of ultraviolet (UV) light downstream of ozone/biofiltration to provide enhanced disinfection and a large-diameter reverse osmosis (RO) membrane for desalination.

Background

UV Disinfection of Drinking Water

Many studies have shown that UV light inactivates bacteria and viruses, however, only recently have studies shown that UV light also inactivates protozoa. Given this biological plausibility of disinfection performance, UV light has received increased attention in the drinking water arena. However, prior to UV's acceptance by drinking water utilities and regulators, a number of operational concerns must be addressed, such as UV lamp and reactor design, UV dose monitoring, and UV sensor placement.

UV Lamp and Reactor Design

Although UV reactors have been used extensively for waste and reclaimed water disinfection, UV treatment of surface water brings different challenges in terms of both scale and its role as a disinfection process. There needs to be an understanding of how UV reactor design (and verification) can be made flexible enough to compliment both small (less than 5 mgd) and large (greater than 50 mgd) systems. A number of lamp types (e.g., low pressure, low pressure high-output, medium pressure and pulsed-UV) are available with different emission spectra and irradiance levels. Research currently underway to equitably compare these lamps is showing that the disinfection achieved by each lamp is similar when results are compared to an equivalent-UV-dose basis. Large systems are needed for drinking water treatment and there is a lack of data for their design or operation.

UV Monitoring

Ultraviolet reactors cannot be directly monitored by either a residual disinfectant or indirectly by changes in water quality characteristics. Thus, UV reactor manufacturers typically characterize UV reactor operation in two ways: biodosimetry or lamp current draw. Using biodosimetry, reactor operation is validated by comparing reactor-seeded organism inactivation with bench-scale results. Alternatively, lamp operation is monitored for UV output (by detection of lamp current draw) and UV transfer (indirect measurement of light irradiance with different sensor technologies). This method of reactor monitoring does not provide a measure of transferred UV dose. It only provides a measure of irradiance at a single point and is blind to certain factors which influence transferred UV dose.

UV Sensor Placement

Actuate sensors are needed in order to insure proper UV disinfection. However, multiple sensor configurations available and the readings from these sensors are not comparable. In addition, the transmissivity of the water may change or the lamp output may degrade over time, leading to erroneous dose measurements.

Large-Scale Reverse Osmosis Desalination

Metropolitan owns and operates five water treatment plants, three of which treat Colorado River water (CRW). Through the use of CRW—which typically has 600 to 700 milligrams per liter (mg/L) of total dissolved solids (TDS)—and other imported water supplies, recent studies have shown approximately $95 million per year in damages to the public and private sectors for every 100 mg/L of TDS over 500 mg/L (Metropolitan 1998)—the U.S. Environmental Protection Agency's secondary, non-health based standard. A planning goal at Metropolitan is to meet or exceed the 500 mg/L TDS secondary standard to minimize the salinity damages and to improve water quality.

Historically, RO systems have not been used for very large plants because of the unfavorable scale-up costs associated with this technology. For example, a 150-mgd RO plant would require about 24,000 standard 8-in.-diameter by 40-in.-long, spiral-wound RO elements. These (smaller) RO elements are ideal for small to mid-size plants, but are not practical for a very large system.

Little additional economy of scale can be achieved for a very large facility needing so many individual pieces; the cost of constructing a 150-mgd plant would be roughly three times the cost of a 50-mgd plant. In contrast, larger RO elements should allow more economical construction of large-scale RO plants.

Project Objectives

The primary objectives of this study were as follows:

- Evaluation of preliminary scale-up issues by assessing operational and water quality needs that impact design criteria for construction of a large-scale UV systems;
- Microbiologically challenge the UV reactor so that its performance can be characterized in terms of transferred UV dose (as related to exact UV dose measured at the bench-scale);
- Monitoring of the UV reactor over a period of testing to evaluate process performance.
- Determine the element productivity, ion selectivity, fouling potential, and cleaning cycle of 16-in. and 8-in.-diameter RO elements; and,
- Provide an economic analysis of a full-scale RO plant utilizing 8-in. versus 16-in. diameter elements

Project Approach

Pretreatment

Pretreatment for both the UV and RO technologies was provided by Metropolitan's demonstration-scale plant in La Verne, California. Water was pre-ozonated (0.95 mg/L ozone) in an over/under-baffled contactor to meet Surface Water Treatment Rule disinfection requirements. Coagulant (2-4 mg/L ferric chloride) and cationic polymer (1.0 mg/L) were fed at a flash-mixer prior to the flocculation basin. The water then passed through a sedimentation basin and a biologically-active anthracite/sand dual-media filter (5.1 gal/min/ft^2 loading rate).

UV Disinfection

A 3-mgd, medium-pressure, enclosed-pipe UV reactor was tested on the demonstration scale. Data on the performance of UV lamp sensors was collected along with water quality data for the water treated by the reactor. Biodosimetry experiments with MS-2 coliphage were also conducted to characterize the UV dose within the reactor.

Reverse Osmosis

A 200-gpm RO unit equipped with two pressure vessels operated in parallel was used to evaluate a large-diameter 16-in. diameter x 60-in. length RO element and a conventional 8-in. x 40-in. element. Both RO elements were spiral-wound and comprised of thin-film composite, polyamide membrane material. The 16-in.-diameter element was a new, experimental RO element with approximately 1,950 ft^2 of effective surface area, approximately 5 times the surface area of a traditional 8-in. element. Both RO elements were operated at 15 gallon/ft^2/day (gfd) flux and 14-15 percent water recovery which are levels that would be seen in a full-scale system operating at 85 percent recovery.

Based on operational data collected using both membrane elements, a hypothetical 185-mgd RO treatment plant was modeled to produce low-TDS water. The location of the desalting facility was assumed to be at an existing conventional water treatment plant with sufficient available space; therefore, only the capital and operation and maintenance costs associated with the RO facility were considered.

Project Outcomes

UV Disinfection

Biodosimetry challenges were conducted with MS-2 coliphage. Challenge results coupled with weekly monitoring of inactivation of heterotrophic bacteria showed that the UV reactor provided adequate disinfection of biofilter effluent, as seen in Figure ES-1. In the range of water quality studied, 75 percent of the reactor capacity (3 of 4 lamps) were able to provide a low-pressure equivalent dose of 50 mJ/cm^2. With 2 to 4 lamps on, bacteria were consistently reduced by more

than 3 $\log_{10}$. However, since these indicators were not monitored during water quality upsets, it is not known if this disinfection level was compromised.

This study showed that if UV technology is to be implemented to treat drinking water, improvements are needed in reactor monitoring and validation techniques. This study began to evaluate correlations between sensor reading and calibrated radiometer reading. Results indicate a linear relationship between the two. However, this relationship needs to be further characterized over a wider range of water quality (e.g., turbidity from 0.1 to 10.0 NTU) to understand sensor reliability for both filtered and unfiltered water applications.

Although this study showed successes in microbial challenges of the UV reactor, results will need to be verified at larger scales. Alternatives to biodosimetry need to be explored so that large California utilities may have other UV reactor dose-characterization options.

Large-Scale Reveres Osmosis Desalination

A 16-in. diameter RO element was operated in parallel to a conventional 8-in. diameter element for over 2,500 hours. The specific flux of the 16-in. element (0.23 gfd/psi) was 20 percent lower than the average specific flux of the 8-in. element (0.28 gfd/psi). Both elements were cleaned twice within 2,500 hours of operation. Both elements removed greater than 98 percent of the influent TDS. Differences in the performance of the two elements were attributed to design issues associated with the 16-in. element: excess membrane leaf length, inability to accurately measure the membrane surface area, and the prototype nature of the membrane manufacturing process.

Results of the potential cost savings associated with the use of 16-in. diameter elements over 8-in. diameter elements for a 185-mgd RO plant are presented in Table ES-1. The large-diameter 16-in. elements are estimated to reduce RO plant capital costs by nearly 24 percent and overall costs (capital costs and O&M costs) by approximately 10 percent (the overall cost savings assumed that a second-generation element with improved flux would be designed). Brine disposal costs were not included in the analysis, but costs would be the same for either membrane size. The reduction in capital costs was mainly due to reducing the overall number of RO skids, as well as reducing the train piping, and support frames. The increased skid capacity

resulted in better economy-of-scale for RO skid instrumentation and membrane feed pumps. The use of large-diameter elements also reduced the overall plant footprint which resulted in a 24 percent savings for the building costs, as well as savings on system-wide controls and electrical equipment.

Conclusions and Recommendations

Conclusions

If UV technology is to be used for municipal drinking water treatment, improvements in reactor monitoring and validation techniques are needed. This study developed a cursory correlation between sensor readings and calibrated radiometer readings which showed a linear relationship over the range studied. This relationship needs to be characterized over a wider range of water quality (e.g., turbidity from 0.1 to 10.0) to understand sensor reliability for both filtered water and unfiltered water applications. Although this study showed successes in microbial challenges of the UV reactor, larger-scale reactors will require validation. Alternatives to biodosimetry need to be explored so that large California utilities may have other UV reactor dose-characterization options.

Large-diameter RO elements look very promising in reducing RO desalination costs for large-scale applications. Evaluation of one of the first 16-in. diameter prototype elements revealed that inefficiencies in the design currently exist. However, as work is continued with membrane manufacturers, the efficiency of the 16-in. element is expected to improve.

Recommendations

It is recommended that this study be followed with research evaluating (1) the effects of water quality and water treatment chemicals on UV disinfection and (2) alternatives to microbial biodosimetry in characterizing UV reactor dose. Characterization of sensor readings to a known standard (i.e., radiometry) should also be continued.

A second-generation 16-in. diameter element should be developed and tested to eliminate the inefficiencies observed in the first prototype element. Improvements in membrane design and optimization of the pretreatment process will help improve membrane productivity and fouling,

which minimizes both capital and O&M costs. An important issue that will need to be addressed in the future is the loading and unloading of the membranes. A dry 16-in.-diameter element weighs approximately 200 lbs and when wetted, an individual element can weigh over 300 lbs.

Table ES- 1. Cost comparison for a 185-mgd desalting system using 8-in. and 16-in. reverse osmosis elements

	Reverse Osmosis Element Size		Savings (%)
Cost Component	8-in.	16-in.	
Annual O&M ($M/year)	19.4	20.8 (19.3*)	-7.2 (0)
Total Capital RO Cost ($M)	170.6	130.2	24
Annual RO Capital Cost ($M/year)	14.9	11.4	24
Total Annual RO System Cost ($M/year)	34.3	32.2 (30.7*)	6 (10)

*Data in parentheses assumes second-generation prototype elements with improved specific flux.

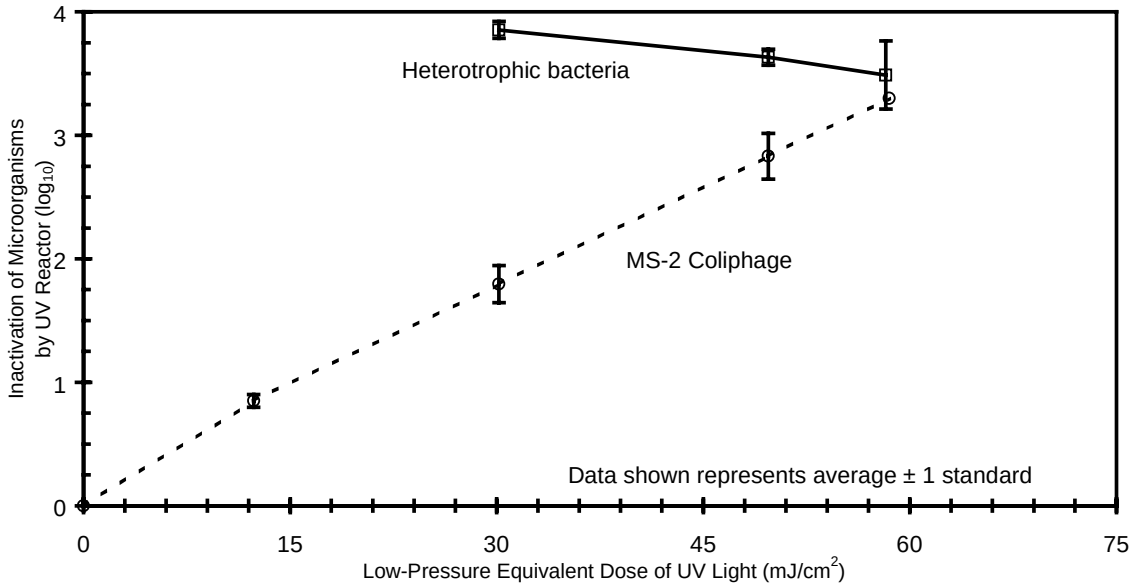

Figure ES-1. Dose response for microbial inactivation using low-pressure equivalent UV dose

ABSTRACT

Drinking water utilities are facing more stringent regulations to provide both adequate disinfection and an aesthetically pleasing water to consumers. This project evaluated a 3 million-gallon-per-day (mgd), medium-pressure ultraviolet (UV) light reactor and a 200 gallon-per-minute, 16-in diameter reverse osmosis (RO) element in an effort to lower the capital costs associated with these technologies. Ultraviolet results showed that adequate disinfection (greater than 3-$\log_{10}$ inactivation of heterotrophic bacteria) could be achieved at turbidities up to 0.3 NTU. During biodosimetry challenges with MS-2 coliphage, a greater than 2-$\log_{10}$ inactivation was accomplished at 75 percent of the reactor's lamp capacity. However, sensor performance was shown to be unreliable. For example, relatively small increases in turbidity from 0.05 to 0.10 NTU caused sensor readings to drop 34 percent.

Parallel testing using a prototype 16-in diameter x 60-in long element and a standard, commercially available 8-in. x 40-in. RO element showed comparable salt rejection (greater than 98.5 percent) between the two element sizes, however the specific flux of the 16-in. diameter element was 20 percent lower than the 8-in. diameter element. This flux difference may have resulted from design or manufacturing inefficiencies of the first-generation prototype and may not be indicative of commercial element performance. Preliminary cost estimates indicated that an approximately 24 percent reduction in RO system capital costs can be achieved mainly through an 80 percent reduction in train piping and vessel support frames. The use of large elements may have many other benefits, including a reduced number of seals (common sources of failures), a smaller footprint, and reduced maintenance requirements.

Keywords:
Reverse osmosis, desalination, ultraviolet light, sensor, disinfection.

INTRODUCTION

The mission of every water utility in the United States is to provide a reliable supply of safe and aesthetically pleasing water using the most cost-effective methods available. In southern California, we face the additional challenges of mitigating the economic impacts of supplies from the Colorado River. As regulations become more stringent, California utilities may need to implement new disinfection and desalting technologies. Two potential technologies for drinking water treatment plant application are ultraviolet (UV) light disinfection and reverse osmosis (RO) desalination. However, both of these technologies are unproven at scales larger than 50 million gallons per day (mgd).

This task evaluated a 3 mgd medium-pressure UV reactor and a 16-in-diameter RO element for large-scale (greater than 50 mgd) applications. Ultraviolet light has been used for decades in the U.S. to disinfect treated waste and reclaimed water for bacteria and viruses. In addition, UV light has been used as a potable water disinfectant in Europe for several years. However, a number of concerns must be addressed before UV becomes well accepted to disinfect treated surface water: (1) the effectiveness of UV against protozoa; (2) the integration of UV disinfection within conventional treatment; and (3) the ability to monitor transferred UV dose to ensure adequate disinfection. Reverse osmosis desalination has been shown effective in reducing salinity to meet secondary regulations governing the aesthetic attributes of treated water, however the high capital and operation and maintenance costs associated with this technology has prevented its widespread use.

Background

UV Disinfection of Drinking Water

Many studies have shown that UV light inactivates bacteria and viruses, however, only recent studies have shown that UV light also inactivates protozoa. Prior to 1998, UV light was not demonstrated as an adequate disinfectant against protozoa (Rice and Hoff 1981, Campbell et al. 1995). Recent data show that this premise was based on inadequate assay techniques, and that protozoa may be easily inactivated by UV light (Clancy et al. 1998, Bukhari et al. 1999). Before UV inactivation of protozoa can be fully understood, an establishment of biological plausibility

(i.e., UV photons react with DNA to prevent replication), treatment efficacy (i.e., the comparison of UV treatment of protozoa versus experiment controls), and UV-dose response is needed.

Combined with the research mentioned above that demonstrates biological plausibility and efficacy, a UV dose-response relationship established by Mofidi et al. (1999) confirms the mode of action and the efficacy of protozoan inactivation. This dose-response relationship helps establish necessary doses to achieve a specified level of treatment. This research also provided evidence that inactivation is not influenced by UV irradiance (i.e., UV dose from continuous-wave UV provides disinfection similar to a UV dose applied with high-intensity, pulsed-UV light).

UV Lamp and Reactor Design

A number of lamp types (e.g., low pressure, low pressure high-output, medium pressure and pulsed-UV) are available with different emission spectra and irradiance levels. Research currently underway to equitably compare these lamps is showing that the disinfection achieved by each lamp is similar when results are compared to an equivalent-UV-dose basis (Linden et al. 2000).

Although UV reactors have been used extensively for waste and reclaimed water disinfection, UV treatment of surface water brings different challenges in terms of both scale and its role as a disinfection process. There needs to be an understanding of how UV reactor design (and verification) can be made flexible enough to compliment both small (less than 5 mgd) and large (greater than 50 mgd) systems. Large systems are needed for drinking water treatment and there is a lack of data for their design or operation. To integrate UV disinfection with conventional treatment, UV reactors will need to be placed post-filtration as a second primary disinfectant. This placement selection is due to water quality needs where a low turbidity and UV-light-absorbing water is provided. A separate primary disinfectant/oxidant (such as free chlorine, chlorine dioxide, or ozone) is needed for preoxidation to assist particle removal (Wilczak et al. 1992) and to provide disinfection assurances to protect public health (e.g., in case of disinfection process failure, there is ample time for backup treatment strategies to be implemented prior to filtration).

UV Monitoring

Also, process monitoring for drinking water treatment differs dramatically from wastewater. For example, wastewater systems monitor UV performance using reductions in coliform density (a monthly geometric mean of coliform bacteria), whereas the mere presence of coliform bacteria causes alarm in drinking water treatment resulting in Surface Water Treatment Rule (SWTR) violations. Other biological surrogates such as aerobic spores and heterotrophic bacteria do not provide a good monitoring tool because of either low densities and long analysis time or lack of presence. This calls for the need to develop reliable monitoring tools for full-scale UV reactors.

UV reactors cannot be directly monitored by either a residual disinfectant or indirectly by changes in water quality characteristics. Thus, UV reactor manufacturers typically characterize UV reactor operation in two ways. Using biodosimetry, reactor operation is validated by comparing reactor-seeded organism inactivation with bench-scale results. In another method, lamp operation is monitored for UV output (by detection of lamp current draw) and UV transfer (indirect measurement of light irradiance with different sensor technologies). This method of reactor monitoring does not provide a measure of transferred UV dose. It only provides a measure of irradiance at a single point and is blind to certain factors which influence transferred UV dose.

UV Sensor Placement

For continuous wave systems, there are several different sensor configurations available. After reactor validation, sensors are either utilized alone to provide an ongoing measure of lamp irradiance or can be combined with a continuous measure of the process water's UV-light transmittance (process water can be pumped to a transmissivity probe). For some systems, the combined readings are used in a feedback loop where lamp intensity in the reactor can be modulated. These readings are also used in conjunction with different lamp cleaning systems, whereby operators can be notified by a low-intensity alarm if the measured irradiance drops below a specified value. The transmissivity/sensor combination compensates for both water quality fluctuations and drops in UV irradiance (whether caused by the end-life of a lamp, or by lamp fouling which has overcome the cleaning system). However, there are still problems in

these sensor designs because sensor response degrades over time due to both fouling and degradation of light detecting material.

The interferences of UV sensors used for either pulsed or continuous-wave lamp monitoring are shown in Figure 1. Sensors are able to detect some changes that will affect UV dose while other factors affecting UV dose remain undetected. As shown in Figure 1, sensors can detect the degradation of light intensity transferred through water due to variable water qualities (represented by the significant changes in the process water UV absorbance at locations A and B) and lamp quartz sleeve fouling (location C). However, hydraulic changes (possibly induced by changes in plant flow) might alter particle trajectory and residence times through a reactor (illustrated by the travel routes D and E) and particles may also block UV light from reaching target organisms (location F). If particles do not pass directly between the lamp and the sensor, particle effects may remain undetected. These phenomenon, which significantly affect delivered UV dose, may be difficult to detect with UV sensors. Because of this degradation, sensors are frequently calibrated using radiometers.

There are many benefits and concerns that arise with the desire to use UV for disinfection of drinking water. As research investigating protozoan disinfection continues, and scale-up issues are addressed, the most needed improvements remain in the area of UV dose monitoring techniques. It is possible that improvements could arise from a combined computational model of fluid dynamics and UV sensors, providing a monitoring tool for conservatively assessing transferred UV dose. This project was conducted to investigate the intermediate stage between bench-scale research (small, controlled batch experiments) and large-scale implementation (greater than 100 mgd installations).

Large-Scale Reverse Osmosis Desalination

A major source of water for the Metropolitan Water District of Southern California (Metropolitan) is from the Colorado River, which typically has 600 to 700 milligrams per liter (mg/L) of total dissolved solids (TDS). The TDS of Colorado River water (CRW) may reach upwards of 750 mg/L in the future (Metropolitan 1998). Recent studies have shown that CRW causes approximately $95 million per year in damages to the public and private sectors for every 100 mg/L of TDS over 500 mg/L (Metropolitan 1998)—the U.S. Environmental Protection

Agency's secondary, non-health based standard. A planning goal at Metropolitan is to meet or exceed the 500 mg/L TDS secondary standard to minimize the salinity damages and to improve water quality.

One option that Metropolitan has been investigating is the use of RO desalination. However, in order to make desalting economical at a large scale (greater than 100 mgd), a breakthrough in RO technology is needed. One potential breakthrough area is the use of large-diameter RO elements (16-in. or larger) over commercially available 8-in. elements. Large diameter elements have the potential to significantly reduce the capital costs of a large-scale RO plant by taking advantage of economies of scale

Metropolitan owns and operates five water treatment plants, three of which treat CRW. Each of the CRW plants (the F. E. Weymouth, Robert A. Skinner, and Robert B. Diemer filtration plants) are 520 mgd in size and use slightly different variations of conventional treatment (most typically rapid mix, flocculation, sedimentation, and dual- or tri-media filtration). The large size of these plants is possible due to favorable economies of scale associated with conventional water treatment systems. Conceptually, the 500-mg/L TDS target could be met by treating a portion of the high-salinity CRW with RO and then blending the desalted water with conventionally treated water. However, given the high TDS rejection of current polyamide RO membranes (greater than 98.5 percent rejection of TDS) and split-flow treatment, the RO system at 85 percent water recovery would need to be at least 185 mgd (permeate flow) to lower the overall TDS from 750 to 500 mg/L.

Historically, RO systems have not been used for very large plants because of the unfavorable scale-up costs associated with this technology. For example, a 150-mgd RO plant would require about 24,000 standard 8-in.-diameter by 40-in.-long, spiral-wound RO elements. These (smaller) RO elements are ideal for small to mid-size plants, but are not practical for a very large system. Little additional economy of scale can be achieved for a very large facility needing so many individual pieces; the cost of constructing a 150-mgd plant would be roughly three times the cost of a 50-mgd plant. In contrast, larger RO elements should allow more economical construction of large-scale RO plants.

Note that the treatment and disposal of the RO brine—a major stumbling block to the actual implementation of large-scale desalting in southern California—is not addressed in this report. However, the brine volumes with large or conventional RO elements would not differ and would not affect the comparison of capital costs.

Project Objectives

UV Disinfection Performance

This study evaluated performance of a 3-mgd UV reactor. This scale was chosen as an intermediate size between the laboratory bench- and pilot-scale (batch volume up to ~200 gallons per minute) and full-scale (greater than 50 mgd).

The primary objectives of this study were as follows:

- Evaluation of preliminary scale-up issues by assessing operational and water quality needs that impact design criteria for construction of a large-scale UV systems;
- Microbiologically challenge the UV reactor so that its performance can be characterized in terms of transferred UV dose (as related to exact UV dose measured at the bench-scale); and,
- Monitoring of the UV reactor over a period of testing to evaluate process performance.

Reverse Osmosis Desalination

The project objectives for the RO study were as follows:

- Determine the element productivity, ion selectivity, fouling potential, and cleaning cycle of the 16-in. and 8-in. RO elements; and,
- Provide an economic analysis of a full-scale RO plant utilizing 8-in. versus 16-in. diameter elements

PROJECT APPROACH

Table 1 provides an overview of the sample type and frequency for the RO study. During the UV study, water quality sampling was completed weekly. All sampling was conducted by

Metropolitan's staff. Inorganic and microbial analyses were analyzed at Metropolitan's Water Quality Laboratory in La Verne, Calif. The water quality constituents for both the UV and RO studies were analyzed according to the methods described in Appendix A. *Standard Methods* (APHA 1998) were used wherever possible.

Research Platforms

Pretreatment

Pretreatment for both the UV and RO technologies was provided by Metropolitan's demonstration-scale plant in La Verne, California. The demonstration plant is located at the F. E. Weymouth Filtration Plant and can provide the operational conditions seen during regular, full-scale, conventional treatment. While the demonstration plant has a design flow of 5.5 mgd, the plant was operated at only 3.0 mgd. Water was pre-ozonated (0.95 mg/L ozone) in an over/under-baffled contactor to meet Surface Water Treatment Rule disinfection requirements (see Figure 2). Coagulant (2-4 mg/L ferric chloride) and cationic polymer* (1.0 mg/L) were fed at a flash-mixer prior to the flocculation basin. The water then passed through a sedimentation basin and abiologically-active anthracite/sand dual-media filter (5.1 gal/min/ft^2 loading rate).

UV Disinfection

The UV reactor, shown in Figure 3, was an enclosed pipe reactor which housed four medium-pressure UV lamps (Sentinel UV Disinfection System; Calgon Carbon Corporation, Pittsburgh, Penn.). The reactor was designed to provide at least 2-log_{10} disinfection of virus in the filtered water at a flow of 3 mgd. The reactor diameter was 24-in. and contained ring- and crescent-baffles as shown in Figure 4. Each lamp was monitored by a sensor inserted into a well protruding from the reactor wall (sensor wells are shown in Figure 5). Figure 6 shows a wiper mechanism inside the reactor. This wiper consists of stainless-steel brushes which surrounded each quartz sleeve. The wiper was programmed to move up and down the sleeve every 5 min of operation.

* Polydimethyldiallylammonium chloride, Agefloc WT-20, CPS Chemical Co., Inc., Old Bridge, New Jersey.

Throughout this study, the UV reactor was operated under the same conditions used in a full-scale treatment plant. Data on the performance of UV lamp sensors was collected along with water quality data for the water treated by the reactor. Biodosimetry experiments were also conducted to characterize the UV dose within the reactor. Biodosimetry experiments were conducted with MS-2 coliphage.

UV Biodosimetry Methods

The reactor was challenged with the a surrogate for human pathogenic viruses, MS-2 coliphage. Figure 7 shows the experiment setup used during MS-2 challenge experiments. During each experiment, water quality and operational data was collected and is presented in Table 2. Typically, 2,000 mL of MS-2 titer (approximately $1x10^{11}$ PFU/mL) was seeded into a carrier water (filter effluent water) and injected upstream of the UV reactor between 2 to 4 hours after backwash of the filter. Once the MS-2 reached the full flow of water going through the reactor (approximately 3.0 mgd or 2,500 gpm), number of MS-2 was diluted to near $5x10^{6}$ PFU/mL. After MS-2 was injected, the full flow of water traveled through one 90^{o} bend, a butterfly valve (valve position between 10 and 20 percent open) and then a pipe diameter change (from 18 in. to 24 in.) before reaching the UV reactor. After UV treatment, pipe diameter was changed back to 18 in. and water samples were collected at the mid-point of another 90^{o} bend. The MS-2 injection port and sample ports were constructed to hydraulically average the flow of MS-2 injected or sampled. Each port was part of a 0.5-in. diameter tube which was inserted into the full diameter of the pipeline. The tube had 0.125-in. diameter holes drilled every 0.5 in. on both sides to disperse or sample MS-2 perpendicular to the direction of water flow. Water velocity per hole for injection and sampling was approximately 4 and 0.02 fps, respectively. All water seeded with MS-2 was disposed of to sanitary sewer.

Reverse Osmosis Unit

A 200-gpm RO unit[†] equipped with two pressure vessels operated in parallel (see Figure 8) was used to evaluate a large-diameter RO element and a conventional 8-in. diameter element. The 8-in. diameter element was a spiral-wound, thin-film composite, polyamide membrane element[‡]

[†] Ionics Ultrapure Water Corp., Watertown, Mass.

[‡] Koch Fluid Systems TFC-4821ULP-400, San Diego, Calif.

with approximately 380 ft^2 of effective surface area. The 16-in. diameter element was a new, experimental spiral-wound RO element[§] with approximately 1,950 ft^2 of effective surface area. The system was equipped with a fully automated control system[**] to collect all pertinent information such as flow, pressure, conductivity, temperature, pH, and turbidity. Both RO elements were operated at 15 gallon/ft^2/day (gfd) flux and 14-15 percent water recovery which are levels that would be seen in a full-scale system operating at 85 percent recovery. Antiscalant[††] was added prior to the 5 µm cartridge filter at a dosage of 1.6 mg/L. No pH adjustment was necessary, because the elements were operated at low water recovery.

Modeling Approach

A hypothetical 185-mgd RO treatment plant was modeled to produce low-TDS water. For the purposes of this paper, the cost of pretreatment (conventional treatment with ozone/biofiltration) was assumed to be sunk and is not presented as part of the overall analysis. The cost information developed for this report is solely for the 185-mgd, RO-treated side-stream (see Figure 9) and does not include brine handling or disposal. The location of the desalting facility was assumed to be at an existing conventional water treatment plant with sufficient available space; therefore, the purchase of additional land was not needed. The amortization rate and period (6 percent and 20 years, respectively) were chosen based on established finance and planning practices at Metropolitan.

The RO plant model was based on the concept of small RO "building blocks," each consisting of 143 pressure vessels per train, using both 8-in. and 16-in. diameter RO elements. This number was chosen based on an RO skid of 5.0 mgd in size using 8-in. x 40 in. elements, which approaches the practical upper limit for such an RO skid. Using 16-in. diameter elements at approximately the same design flux, the individual RO skids increased in size to 16.8 mgd/skid. These building blocks were then replicated to treat the entire desalted flow. Thus, the RO plant costs would scale linearly, and economy-of-scale savings would only be realized for site work and system-wide controls.

[§] Koch Fluid Systems SE 16060ULP, San Diego, Calif.

[**] PanelView 1000, Allen Bradley, Milwaukee, Wis.

[††] Permacare, Permatreat 191, Fontana, Calif.

The RO plant and membrane performance parameters used for the cost estimate are listed in Table 3 (CH2M Hill 2000). Salt rejection was assumed to be equivalent between the 8-in. and 16-in. diameter elements. However, the specific flux (flux divided by the net driving pressure) for the 16-in. prototype element was shown to be approximately 24 percent lower than that for a commercially available 8-in. RO element (see following discussion). Assuming no changes in capital equipment are needed, this would result in a 20 percent increase in applied feed pressure. It was also assumed that with further development, a second-generation, 16-in. diameter RO element could be manufactured such that the specific flux is comparable to an 8-in. RO element. Applied pressure was calculated based on a 750-mg/L TDS influent at 64°F (18°C)—the annual median water temperature. Energy costs were calculated based on the applied feed pressures for both the first- and second-generation 16-in. RO elements (168 and 140 psi, respectively).

No RO brine treatment or disposal costs were assumed for this study; however, brine costs would be the same for RO systems using large- or conventional-diameter elements. It should be noted that for a 185-mgd permeate capacity RO plant operating at 85 percent water recovery, the resulting brine stream would be approximately 33 mgd. This level of water loss in the arid Southwest would be unacceptable. Therefore, further brine treatment to increase the overall system water recovery would need to be instituted. Furthermore, no additional brine line capacity to transport even a fraction of this brine stream is in existence; therefore, new brine lines would need to be constructed. Each of these additional costs would substantially increase the total desalting facility cost.

PROJECT OUTCOMES

UV Disinfection

The large-scale, medium-pressure UV lamp reactor was evaluated over a 4.5-month period (3,288 hours) using conventionally pre-treated water. The water treated at the plant was a blend of California State Project water (SPW) and Colorado River water (CRW). Water quality parameters and the range of values measured during the test period is presented in Table 4 and treatment plant operational data is presented in Table 5. As mandated by the SWTR (USEPA 1989), conventional treatment of surface water is required to achieve 3-$\log_{10}$ removal/inactivation of *Giardia* cysts and 4-$\log_{10}$ removal/inactivation of virus. The most

significant barrier to pathogens in conventional treatment is through physical removal. The SWTR credits properly operating treatment plants with 2.5-$\log_{10}$ removal of *Giardia* cysts and 2.0-$\log_{10}$ removal of viruses (direct filtration is credited with less removal). The remaining 0.5-$\log_{10}$ reduction of *Giardia* cysts and 2.0-$\log_{10}$ reduction of virus may be achieved through disinfection. The treatment plant supplying water to the UV reactor in this study (illustrated schematically in Figure 2) consistently met these requirements by providing a filtered water quality consistently less than 0.3 NTU and by using an ozone dose of 1.1 mg/L to achieve a 1.3 ± 0.5 $\log_{10}$ inactivation credit of *Giardia* cysts and a 2.6 ± 1.2 $\log_{10}$ inactivation of virus. Ozone served two purposes: (1) to provide adequate disinfection to meet SWTR guidelines and (2) to provide a pre-oxidant so that the treatment plant's filtration process continued to operate properly, only allowing low levels of particles (turbidity) to pass.

The filtration process downstream of ozonation served two purposes: (1) to remove particulates and (2) as a biological support for removal of biodegradable ozonation byproducts. The UV reactor was operated downstream of biologically active filtration (biofiltration) to act as a disinfectant for bacteria that slough off of the biofilter. This location is the most appropriate to apply UV light as the water quality is characterized by low turbidity (turbidity may block or scatter UV light before it reaches target microorganisms) and high UV transmittance. The UV reactor was evaluated to identify scale-up issues with a two-fold experimental plan: (1) with live microorganism challenges and (2) by continuous monitoring of operational and water quality parameters.

In the microorganism challenges, live MS-2 coliphage were seeded into the system to understand the transferred UV dose within the reactor. This practice, termed biodosimetry, was conducted in parallel with bench-scale collimated beam disinfection of the MS-2 to fully understand the reactor's operating UV dose. The biodosimetry work characterized the UV dose per lamp at the optimum flow rate of the reactor.

Continuous monitoring of the UV reactor over the study period allowed the identification of two factors which affected UV reactor performance: (1) hardware issues (i.e., effects on treatment due to issues related to process hardware) and (2) water quality issues (i.e., water quality effects on treatment).

Biodosimetry Characterization of UV Reactor

As documented in the standard set by the German Association on Gas and Water, the characterization of dose for UV reactors can only be reliably accomplished by microbiological examination (DVGW 1997), otherwise known as biodosimetry. Usually, this is done by spiking microbial surrogates to measure disinfection. One of the challenges of operating a large-scale UV reactor is that this technique is impractical. However, large-scale applications (greater than 50 mgd) would require reactor sizes which would make this technique impractical scale-wise. Another likely problem is that the volume of test water spiked with microorganisms may be too great to manage from a discharge point of view. Unlike wastewater treatment, filtered drinking water will not have natural microbial indicators downstream of filtration (necessitating the use of artificially seeded surrogates), making this a complex issue to resolve.

Biodosimetry challenge tests were conducted in triplicate. Each test was comprised of: (1) a bench-scale characterization of the dose-response of MS-2 coliphage to an accurately measured UV dose (a low-pressure UV lamp was used for collimated beam work) and (2) a UV reactor challenge with MS-2. Bench-scale dose-response experiments and UV reactor challenge tests were conducted on the same day. Figure 10 summarizes results from the three bench-scale collimated beam experiments. The bench-scale, collimated-beam experiments provided a coefficient of determination (R^2) = 0.99 indicating a linear correlation between MS-2 inactivation and UV dose shown in Figure 10. Bench-scale, low-pressure UV inactivation of MS-2 allowed data from the full-scale MS-2 biodosimetry tests to be plotted against a low-pressure equivalent UV dose, as shown in Figure 11 (heterotrophic bacteria data shown in Figure 11 will be described later). During the experiments, and for the range of water quality evaluated, the UV reactor was able to provide a low-pressure equivalent dose of 12, 30, 50, and 58 mJ/cm^2 for 1, 2, 3, and 4 lamps operating, respectively. Due to equipment problems, only one test was performed with 4 lamps (note the absence of standard deviation bars).

UV Process Performance

Throughout the study, there were a number of process upsets due to both mechanical problems with UV reactor hardware and water-quality-related problems due to process upsets at the water treatment plant.

Hardware Issues

During this evaluation the there were several concerns with UV reactor performance attributed to hardware-related issues. Figure 12 shows the sensor readings on the 4 UV lamps throughout the study. The UV lamps were rated for a 3,000 hr life, however, they routinely failed before their rated life. Initial lamp failures (taking reactor down-time into consideration) were recorded at 1,023 hr (lamp 3) and at 1,450 hr (lamp 1). After almost 2,000 hr into the study, all 4 lamps were replaced. After lamp replacement, capacitor banks started to fail which, in turn, caused the lamps to fail (capacitor failures caused lamps to fail at 182 hr for lamp 2 [test time of 2,136 hr] and 751 hr for lamp 4[test time of 2,784 hr]). Another issue raised by the lamp failures was the need to have replacement lamps on-site. After failure of lamp 3 (at 1,023 hr), a replacement lamp was not available until 2,000 hr into the study due to delays in ordering through the manufacturer.

Table 6 summarizes sensor performance for the different operational periods of the study and Figure 13 shows changes in water quality. Investigating sensor performance across the study period, it was evident that decreases seen in sensor performance (e.g., from 0 to 768 hr) were not due to the water quality parameters measured. From 0 to 768 hr, water quality remained relatively constant while lamp sensor readings fluctuated greatly (e.g., lamp 1 ranged from a high of 45 to a low of 24 percent scale). The high sensor reading data for all the lamps were nearly double that of the low reading for this initial period of the study. From 792 hr to the end of the study, the sensor readings remained variable but were lower than the initial study period described above (e.g., lamp 1 ranged from a high of 35 to a low of 17 percent scale). Reduction in lamp sensor readings shown in Table 6 do not include lamp outages.

The first 768 hours of the study showed both: (1) significantly different sensor readings and (2) a drop in each sensor reading over time. To better understand the cause behind these effects, the sensors were manually switched for a brief time period. The results of this switch presented in Table 7. During this switch, the position of sensor 1 was switched with sensor 2 (sensor 2 was placed in sensor well 1 to read lamp 1, and sensor 1 was placed in sensor well 2 to read lamp 2) and the position of sensor 3 was switched with sensor 4, then sensors were placed back in their appropriate wells. Switching sensors 1 and 2 showed that both sensors kept similar readings no

matter the well position (sensor 2 read significantly higher than sensor 1 in both positions). Although there were significant changes in sensor readings for sensors 3 and 4, a similar effect occurred (sensor 4 read significantly higher than sensor 3 in both positions). This result indicates that the difference in reading from one sensor to the next may be due to sensor hardware. If there was a water quality or lamp fouling issue causing differences between sensor readings, the readings would be well-specific, and not sensor-specific. The data seem to indicate that the drop in sensor readings over the first 768 hr was not due to lamp fouling or lamp age, but possibly due to sensor age. This indication comes from 1,300 to 2,000 hrs where the sensor reading for lamp 2 is stable (except for known water quality changes) and has recovered to its reading at 0 hr.

Sensor readings presented in this report represent a percent of the total irradiance (expressed as milliwatts/cm^2 [mW/cm^2]) for each sensor. Therefore, if a sensor reads 100 percent, the true meaning of that data should be 100 percent of maximum irradiance. The manufacturer indicated that 100 percent of the maximum irradiance for the individual sensors should be 3 mW/cm^2. To characterize sensor readings to a reliable and repeatable measure, a radiometer with a fiber-optic probe and detector (IL1400 with FF02500 fiber optic cable & adapter, SEL240/G detector calibrated to NIST standards; International Light, Newburyport, Mass.) was used. This allowed an understanding of the relationship between sensor reading and a calibrated, radiometer-measured irradiance. Although the sensors and the radiometer have a theoretically different acceptance angle (±6.2 degrees for the sensors and ±5.0 degrees for the radiometer configuration used), the sensor and radiometer probes were placed at the exact same location in the sensor well to get the best possible comparison between the two light-measurement technologies. Because the radiometer would become saturated and damaged by continuous exposure to UV light, it was used only as a check against the sensor readings twice a week. This comparison started late in the study, so only a few data points are available for discussion in this report.

Figure 14 illustrates the relationship that was found between the UV sensor reading for each lamp and the reading provided by a calibrated radiometer. These data represent readings across a small range and it is unknown if the relationship across the entire scale is linear. Examining the linear regression of data for each of the four sensors, it is apparent that the slope of each relationship is similar. However, each sensor/radiometer regression provides different

y-intercept values. According to sensor relationships with the radiometer, the sensors' maximum irradiance detection may be above the manufacturer's rating of 3 mW/cm^2.

Water Quality Issues

Data showing the effect of changing water quality on sensor performance is summarized in Table 6 and in Figure 15. During the study period (Figure 12) there were three separate occasions of process upset recorded by the sensors—one due to failure of the chemical feed pumps (see note A), one due to shutdown of the ozone system (see note D), and one due to a change in source water quality (see note H). Table 6 indicates that due to the loss of chemical feed, the median sensor readings for all lamps dropped from between 41 to 43 percent of the median reading for the previous 768 hr. The loss of pre-oxidation caused the sensors to drop between 43 to 65 percent of the median reading for the remainder of the study (from 792 hr to the end of the study). Figure 15 characterizes the effect of water quality on readings for sensor/lamp combination 4. It can be seen by this data that the wide range in the sensor scatter occur during both normal process operation and stressed operation resulting from process upset. Because of this scatter, sensor response was not seen to be linearly related to water quality.

After realizing the sensitive relationship between sensor reading and changes in pre-treatment, a study was conducted to monitor sensor performance after a loss of preoxidation. Figure 16 and Table 8 summarizes sensor and water quality data for this 24-hr period. During the study, the water pH was 8.4 and the temperature was 55°F. The study was conducted by deliberately turning off the ozone generator at the head of the treatment plant (at time –5 min). The theoretical detention time between the ozone contactor and the filter effluent is 250 min, however, multiplying this by the hydraulic performance ratio (T_{10}/T) of the plant processes this time is reduced to 88 min. Figure 16 (a) and (b) are sectioned into five periods. Period *A* (from 0 to 175 min) indicates normal operation while periods *B* through *E* represent effects due to the loss of ozone. Throughout the study, filter effluent turbidity remained below 0.12 NTU and the UV transmittance (at 254 nm) only dropped from 95 to 92 percent. During period A, it can be seen that sensor readings (although significantly different) were stable, along with water quality.

During Periods *B* through *E*, the sensors responded similarly to the changes in water quality. Period *B* shows the first dramatic increase in particles passing through the filter. Turbidity and

particle counts increase 46 and 40 percent, respectively. Readings for sensors 1 through 4 decreased by roughly 15 percent. Period *C* showed relatively no change in water quality (turbidity and particles increased 4 and 12 percent, respectively) or sensor readings (all sensors decreased by 2 percent). Period *D* showed an even more dramatic change in water quality than was seen in period *A* (turbidity and particles increased 43 and 70 percent, respectively). Performance during period *D* was characterized by a 17 percent decrease in reading for the sensors. During period *E* there was no large change in turbidity particle counts, but readings for sensors 1 through 4 dropped by approximately 5 percent. Throughout the study, UV transmittance decreased by less than 3 percent while turbidity and particle counts increased by 117 and 158 percent, respectively. The increase in particles through the UV reactor resulted in a dramatic decrease in sensor readings, with a 34 percent net drop of each sensor reading.

Effect of UV Treatment on Water Quality

Throughout the study, inactivation of heterotrophic bacteria was monitored through the UV reactor with results presented in Figure 17. The average number of bacteria sloughing off of the biofilter was 1.5×10^4 CFU/mL. Across the study, the reduction of bacteria by UV treatment was seen to be 3.4 ± 0.5 $\log_{10}$ (average ± standard deviation). This provided 14 ± 20 bacteria in the UV-treated water (maximum value of 67 on day 2,352 and minimum value of 1 on days 984 and 1,824. Water temperature was seen to increase slightly (average of 0.08^{o}F) by UV treatment (temperature measured before and after the reactor each day). Figure 11 (previously used to describe MS-2 inactivation) shows the inactivation of bacteria achieved according to the number of lamps which were on (throughout the study, no data were collected for 1 lamp on). When either lamps 2, 3, or 4 were on, a greater than 3 $\log_{10}$ inactivation of bacteria was achieved. The average power draw per lamp to provide this treatment ranged from 3.2 to 3.7 kWh.

Reverse Osmosis

Operational Data

Table 9 summarizes the operational data for the 8-in. and 16-in. elements. The specific flux over the initial 100 hrs of operation for the 8-in. RO element (0.227 gal/ft^2/day/psi) was observed to be an average of 20 percent higher than the 16-in. RO element (0.283 gal/ft^2/day/psi) (see Figure

18). Over time, the difference in specific flux between the 16-in. and 8-in. RO elements increased to greater than 24 percent due to a higher fouling rate for the 16-in. element.

Based on daily conductivity readings, the salt rejection for both elements was comparable (see Figure 19). Table 10 shows the percent rejection data for selected analytes. Overall TDS rejection for the 8-in. and 16-in. elements was 98.7 and 98.4 percent, respectively. However, data analysis for aluminum and iron was problematic because of their relatively low concentrations in the influent.

Performance Difference

Differences in the membrane flux between the 8-in. and 16-in. diameter elements were attributed to one or more of the following: (1) membrane material, (2) effective surface area, and/or (3) membrane leaf length. Small quality variations in the membrane material resulting from the manufacturing process are expected and can account for a five percent difference in membrane performance. The effective surface area of the element is a critical value that directly affects the calculation of the specific flux. Although the actual membrane surface area that is used to manufacture an element is well known, the effective surface area of the membrane after gluing is uncertain. Typically, a five percent reduction in the effective surface area can be assumed after gluing of the membrane. However, because the 16-in. diameter is a prototype element, assuming a five-percent reduction in actual effective service area may be inaccurate. For this report, the effective surface areas of both the 8-in. and 16-in. elements were assumed to be five percent less than the manufacturers' specifications (380 ft^2 for the 8-in. and 1,948 ft^2 for the 16-in. element).

The most significant difference between the two elements was determined to be the leaf length. The 8-in. element had a leaf length of 90 in., and the 16-in. element had a leaf length of 130 in. As the leaf length increases, the water must travel a longer distance to reach the permeate tube. As a result, the longer leaf length element requires more pressure than the shorter leaf length element at the same flux and recovery to drive the water through the semi-permeable membrane to the permeate tube. It was hypothesized that the difference in the leaf length was the major contributing factor in the lower specific flux of the 16-in. element.

Differences in Membrane Fouling

Both the 8-in. and 16-in. elements were chemically cleaned at 1,130 hrs of operation after a 17 percent reduction in flux had been observed for the 16-in. element (see Figure 18) and a greater than 15 psi differential pressure for the 8-in. element (see Figure 20). The membranes were cleaned with sequential applications of acidic solution (citric acid adjusted to pH 2.0 to 2.5) and caustic solution (equal parts Na-EDTA, sodium tripolyphosphate, and trisodium phosphate adjusted for pH 10.0 to 10.5). The flow rate during the cleaning cycle was 60 gpm for the 16-in. element and 30 gpm for the 8-in. element. Because of operational limitations of the cleaning-skid pump, the flow rate for the 16-in. element was not proportional to that of the 8-in. element (the manufacturer recommends a cleaning flow rate of 160 gpm for the 16-in. element). After this first chemical cleaning, a recovery in performance for the 16-in. element was not observed. The ineffectiveness of the chemical cleaning was attributed to the low crossflow rate through the 16-in. element during the cleaning cycle.

Both membranes were cleaned for a second time at 2,466 hours of operation after a significant decrease in specific flux for the 16-in. element and a greater than 15 psi differential pressure for the 8-in. element was observed. The same cleaning chemicals were used for the second cleaning. However, the 8-in. and 16-in. elements were cleaned separately, and the maximum flow rates through each element was increased to 31 gpm and 135 gpm, respectively. Data taken after the second chemical cleaning indicated a 20 percent recovery in flux for the 16-in. element and an 80 percent reduction in differential pressure for the 8-in. element.

Operational data and water quality data indicate that biological fouling of the RO system may have occurred. An increase in the differential pressure and constant flux is normally indicative of early stages of biofouling. In the initial stages of biofouling, bacteria can plug the feed spacers between the membranes and cause an increase in fluid frictional drag, which in turn increases the differential pressure. As the biofouling continues, a gradual decrease in water flux will then be observed. The operational data for both elements were consistent with this type of membrane fouling. In addition, high counts of HPC bacteria in the RO feed and permeate was observed (average of 4800 counts/mL and 34 counts/mL [combined permeate], respectively), which further indicates that the fouling may have been biological. Biofouling of the RO

membranes, however, is not necessarily due to the design of the elements or membrane characteristics but is more a function of the pretreatment. Improvements in the pretreatment step may eliminate or minimize the fouling of the RO membranes.

Cost Model Results

Table 11 shows the capital cost assumptions developed for this paper. Installed membrane costs ($650/element and $3,350/element for the 8-in. x 40-in. and 16-in. x 60-in. RO elements, respectively) and pressure vessel costs ($1,540 and $4,950 for the 8-in.-diameter and 16-in.-diameter pressure vessels, respectively) were based on original equipment manufacturers' cost estimates (Casey 2000, Eisberg 2000). These capital costs for RO include a $50 and $400 installation cost for 8-in. and 16-in. elements, respectively, and a $140 and $450 installation cost for 8-in. and 16-in. pressure vessels, respectively. All other costs were developed by CH2M HILL through either verbal quotes (e.g., membrane feed pumps), internal cost data (e.g., skid piping), or through a proportion of the overall plant costs (e.g., electrical components and plant controls). Operation and maintenance (O&M) costs were based largely on standard cost estimates (e.g., labor) or water quality requirements (e.g., chemical costs were estimated based on CRW water quality data to lower the influent pH to 7.0 and readjust the permeate pH back to 8.3) (see Table 12).

Table 13 shows a breakdown of the capital costs for a 185-mgd permeate capacity RO plant using both 8-in. and 16-in. elements. The overall capital cost savings for an RO system using 16-in.-diameter elements was 24 percent. This reduction in capital expenditures was largely a result not only of reducing the overall number of RO skids (37, 5.0-mgd skids using 8-in. elements versus 11, 16.8-mgd skids using 16-in. elements), but also of reducing the train piping, a cost savings of 80 percent per RO skid. The increased, rated skid capacity also resulted in substantial costs savings in RO skid instrumentation and membrane feed pumps for the overall plant. It should be noted that not only were there fewer membrane feed pumps using 16.8-mgd skids, but each 19.8-mgd feed pump (16.8-mgd permeate flow divided by 85 percent water recovery) was proportionally less expensive on a cost per volume treated per day basis than for a 5.9-mgd feed pump (5.0 mgd/85 percent).

Other capital cost savings associated with using large-diameter elements in greater capacity trains were a reduced plant footprint that resulted in reduced building costs (24 percent savings), as well as savings on system-wide plant controls and electrical equipment (28 percent reduction for each) (see Table 13). The only negative economy-of-scale was for the capital costs of installing the 16-in. RO elements. While the 16-in. membranes are competitive on the basis of cost per square-foot of membrane ($1.53/ft^2 for 16-in. x 60-in. elements versus $1.58/ft^2 for 8-in. x 40-in. elements), the increased cost of installing the elements ($400/16-in. element versus $50/8-in. element) negated this positive economy of scale. However, the cost for installing 16-in. RO elements is only an approximation and as more experience with large-diameter elements is gained, the cost to install large-diameter elements may decline.

Table 14 shows the total cost for a 185 mgd permeate capacity RO facility. When using the actual RO performance data collected during this study, the O&M costs were 9 percent higher for the 16-in. RO system. The higher O&M costs resulted from the 20 percent higher applied feed pressure required by the 16-in. system (168 psi versus 140 psi for the 8-in. RO system) that resulted in a concomitant increase in energy consumption. However, when equal specific fluxes were assumed (0.28 gfd/psi), the O&M costs did not change significantly using either membrane size. This resulted, in part, from the same amount of water needing to be pumped at the same pressure regardless of membrane size.

A slight decrease in membrane replacement costs was observed, but this represented only a small fraction of the overall O&M costs. It may be argued that O&M labor may decline slightly using large-diameter elements because they have fewer O-rings, a common source of failure that requires labor-intensive maintenance. Alternatively, using large-diameter elements that cannot be manually handled may increase the labor cost. Both of these considerations were not used in determining the O&M labor component. An important issue that was not addressed in this paper is the loading and unloading of the membranes. A dry 16-in. diameter element weighs approximately 200 lb and when wetted, an individual element can weigh over 300 lb. In order for these large-diameter elements to be used at the full scale, it will be important to design a method of easily removing and loading them that is not labor-intensive.

When equal RO element performance was assumed, the O&M fraction of the total plant cost was approximately 57 and 63 percent for the 8-in. element and 16-in. element membrane systems, respectively. Given that the O&M for a large-scale desalination plant did not change significantly when using second-generation, 16-in. diameter elements, the overall RO plant costs, both capital and O&M, decreased by only 10 percent (see Table 14). However, when using first-generation elements with element inefficiencies, the overall RO plant costs decreased by only 6 percent.

CONCLUSIONS AND RECOMMENDATIONS

Conclusions

UV Disinfection of Drinking Water

The challenge with providing water which meets all State and Federal regulations for disinfection and DBPs is that operators need treatment processes which can be reliably monitored both in the short- and long-term period. When short-term water quality episodes occurred (e.g., a loss of preoxidation or chemical feed, or a source water change), sensor response was not acceptable from an operations-monitoring standpoint. Although the filtered water turbidity never increased past 0.3 NTU, dramatic drops in sensor output (as much as 34 percent) were noticed. Long-term changes in both sensor performance and equipment failures caused the reactor to either: (1) provide a level treatment which was not fully understood (gradual drop in sensor readings were likely due to sensor performance and not fouling or changes in water quality) or (2) cause the reactor to be taken off-line.

Biodosimetry challenges and routine monitoring inactivation of heterotrophic bacteria showed that the reactor provided adequate inactivation of these organisms. In the range of water quality studied here, 75 percent of the reactor capacity (3 of 4 lamps) was able to provide a low-pressure equivalent dose of 50 mJ/cm^2. With either 2 or 4 lamps on, bacteria were consistently reduced by more than 3 $\log_{10}$. However, it is not known how this disinfection was compromised during the episodes of significant decrease in sensor performance (MS-2 and bacteria data were not collected during episodes where sensor readings were compromised).

If UV technology is to be used for municipal drinking water treatment, improvements in reactor monitoring and validation techniques are needed. This study developed a cursory correlation between sensor readings and calibrated radiometer readings, which showed a linear relationship over the range studied. This relationship needs to be characterized over a wider range of water quality (e.g., turbidity from 0.1 to 10.0) to understand sensor reliability for both filtered water and unfiltered water applications. Although this study showed successes in microbial challenges of the UV reactor, larger-scale reactors will require validation. Alternatives to biodosimetry need to be explored so that large California utilities may have other UV reactor dose-characterization options.

Large-Diameter RO Element

The 16-in. diameter RO element was a prototype that requires changes in the design to improve flux when compared to a commercially available 8-in. diameter element. The average specific flux of the 16-in. and 8-in. element during 2,500 hours of continuous operation was 0.28 and 0.21 gal/ft^2/day/psi, respectively. The cleaning cycle for both elements was approximately 1 to 2 months when using conventional treatment with ozone/biofiltration and no chloramines. With continued improvements in the leaf length, membrane surface area estimation, and overall manufacturing of the 16-in. element, most of the inefficiencies are expected to be minimized. In addition, as large-diameter elements are mass-produced, the cost of the elements is expected to decline. Both elements exhibited excellent rejection properties and removed greater than 98 percent of the influent TDS.

The use of large-diameter membrane elements is estimated to reduce large-capacity RO plant capital costs by nearly 24 percent and unit production costs by approximately 10 percent. The costs excluded brine disposal, however, this cost would be the same using either RO element size. The reduction in capital expenditures was largely a result of reducing the overall number of RO skids, as well as reducing the train piping, and support frames. The increased skid capacity also resulted in substantial costs savings in RO skid instrumentation and membrane feed pumps. Other capital cost savings associated with using large-diameter elements included a reduced plant footprint that resulted in reduced building costs (24 percent savings), as well as savings on system-wide plant controls and electrical equipment (28 percent reduction for each). Further

research and development will help to improve the performance of the large-diameter elements and reduce costs for large RO systems.

Commercialization Potential

UV Disinfection

Currently, UV reactors are manufactured by a number of companies and are now being marketed in the drinking water industry. However, due to shortfalls in technology performance (outlined in this report), widespread use of UV treatment in drinking water may not spread quickly.

Large-Diameter RO Elements

Currently, large-diameter elements of 16-in. or larger are not commercially available due to the following factors: 1) a high demand for large-diameter elements currently does not exist, 2) membrane manufacturers do not have the necessary capital equipment to mass-produce large elements, and 3) difficulties in handling larger-diameter elements must be resolved. However, as desalination plants continue to grow in number and capacity to meet growing demand and limited water resources, large-diameter elements are expected to become more attractive and cost-effective than conventional RO elements.

Recommendations

It is recommended that this study be followed with research evaluating (1) the potential interference of water treatment chemicals (e.g., coagulant residuals) on UV disinfection during water quality challenges and (2) alternatives to microbial biodosimetry in characterizing UV reactor dose. Characterization of sensor readings to a known standard (i.e., radiometry) should also be continued.

Additional applied research is still needed to further optimize the RO process following conventional treatment or conventional treatment with ozone/biofiltration. A second-generation 16-in. diameter element should be developed and tested to eliminate the inefficiencies observed in the first prototype element. Improvements in membrane design and optimization of the pretreatment process will help improve membrane productivity and fouling, which minimizes both capital and O&M costs.

An important issue that will need to be addressed in the future is the loading and unloading of the membranes. A dry 16-in. diameter element weighs approximately 200 lbs and when wetted, an individual element can weigh over 300 lbs. A 150 mgd plant will contain over 5,000 elements, and the handling of these membranes can significantly increase O&M costs. Specialized mechanical equipment should be developed to easily handle these large-diameter elements.

Benefits to California

UV treatment of drinking water could be a great benefit to California by allowing a relatively low-cost technology to provide enhanced disinfection and protection of public health. However, significant advances are needed in UV sensor technology, UV dose characterization (i.e., validation techniques such as biodosimetry), and methods in combining these two issues to provide consistent, reliable reactor monitoring before safe and reliable implementation can be expected.

The development of large, 16-in. diameter elements will benefit the entire state of California by lowering the cost of desalination and reducing the energy requirements to treat brackish water. The successful development of these large-diameter elements will help to significantly lower cost of new, large-scale desalination facilities (greater than 100 mgd) by taking better advantage of economies of scale.

REFERENCES

APHA (American Public Health Association), AWWA (American Water Works Association) and WEF (Water Environment Federation). 1998. *Standard Methods for the Examination of Water and Wastewater.* 20th ed. Edited by L.S. Clesceri, A.E. Greenberg, and A.D. Eaton. Washington, D.C.: APHA.

Bartels, C.R., C.J. Gabelich, T.I. Yun, M.R. Cox, J.F. Green. 1999. Effect of Pretreatment on Reverse Osmosis Performance for Colorado River Water Desalination. In *Proc. IDA World Congress on Desalination and Water Reuse. San Diego, Calif.*: IDA.

Bolton, J.R. *Ultraviolet Applications Handbook*, 1st Ed. 1999, Ayr, Ontario, Canada, Bolton Photosciences, Inc.

Bukhari, Z.; Hargy, T.M.; Bolton, J.R.; Dussert, B.; and Clancy J.L. *Medium-Pressure UV for Oocyst Inactivation*. Jour. AWWA, 91:3:86 (1999).

Campbell, A.T.; Robertson, L.J.; Snowball, M.R.; and Smith, H.V. *Inactivation of Oocysts of Cryptosporidium parvum by Ultraviolet Irradiation*. Water Res., 29:11:2583 (1995).

Casey, W. (Koch Membrane Systems). Personal communication (Dec. 2000).

CH2M HILL, Inc. Unpublished data prepared for Metropolitan (Dec. 2000).

Clancy J.L.; Hargy, T.M.; Marshall, M.M.; and Dyksen, J.E. *UV Light Inactivation of Cryptosporidium Oocysts*. Jour. AWWA, 90:9:92 (1998).

DVGW (Deutscher Verein des Gas- und Wasserfaches e.V. UV-Desinfectionsanlagen fur die Trinkwasserversorgung – Anforderungen und Prufung. October 1997. Postfach, Bonn, Germany.

Eisberg, D. (Progressive Composite Technologies). Personal communication (Dec. 2000).

Gabelich, C.J.; Bartels, C.R.; Yun, T.I.; & Green, J.F. 2000. Comparing Treatment Strategies for Surface Water Desalting. In *Proc. AWWA Annual Conference, Denver, Colo.*

Gabelich, C.J.; Yun, T.I.; Bartels, C.R.; & Green, J.F. (in press). Non-Thermal Technologies for Salinity Removal: Final Report. AWWA & AWWARF, Denver, Colo.

Linden, K.G.; & Mofidi, A.A. *Unsolicited proposal submitted to AWWARF: Disinfection Efficiency and Dose Measurement for Medium Pressure and Pulsed-UV Disinfection Systems*. (1998).

Linden, K.G.; Mofidi, A.A.; Jin, S.; Chou, C.I.; Baribeau, H.; Hwang, C.; & Guo, C. (2000) Disinfection Efficiency and Dose Measurement in Medium-Pressure and Pulsed-UV Systems. AWWA Annual Conference and Exposition, Denver, Colo., AWWA.

Malley, J.P.; Shaw, J.P.; & Ropp, J.R. (1995) Evaluation of By-Products Produced by Treatment of Groundwaters With Ultraviolet Irradiation. Denver, CO, American Water Works Association Research Foundation.

Malley, J.P.; Margolin, A.; Mofidi, A.A.; Crozes, G.; and Linden, K.G. *Solicited proposal submitted to AWWARF: Inactivation of Pathogens by Innovative UV Technologies*. (1999).

Metropolitan Water District of Southern California and U.S. Department of the Interior, Bureau of Reclamation. 1998. *Salinity Management Study; Final Report.* Sacramento, Calif.: Bookman-Edmonston Engineering.

Mofidi, A.A.; Baribeau, H.; and Green, J.F. *Inactivation of Cryptosporidium parvum With Polychromatic UV Systems*. Proc. 1999 AWWA WQTC, Tampa, Fla.

Mofidi, A.A.; Bartels, C.R.; Coffey, B.M.; Ridgway, H.F.; Knoell, T.; Safarik, J.; Ishida, K.; & Bold, R. 2000. Ultraviolet Irradiation as a Membrane Biofouling Control Strategy. In *Proc. AWWA Annual Conference*, Denver, Colo.

Rice, E. W., and Hoff J.C. *Inactivation of Giardia lamblia Cysts by Ultraviolet Irradiation*. Appl. Environ. Microbiol., 42:3:546 (1981).

USEPA (United States Environmental Protection Agency) Drinking Water; National Primary Drinking Water Regulations; Filtration and Disinfection; Turbidity, Giardia lamblia,

Viruses, Legionella, and Heterotrophic Bacteria; Final Rule. *Federal Register* 54:124:27486-27541. (1989)

Wilczak, A.; Howe, E.W.; Aieta, E.M.; and Lee, R.G. How Preoxidation Affects Particle Removal During Clarification and Filtration. *Jour*. AWWA, 84:12:85 (1992).

GLOSSARY

ATCC	American Type Culture Collection
$CaCO_3$	calcium carbonate
Commission	California Energy Commission
cm	centimeter
CRW	Colorado River water - the water source of Lake Mathews, California, the southern terminus for the Colorado River aqueduct system
R^2	coefficient of determination
CFU/mL	colony forming units per milliliter
d	day
^oC	degrees Celsius
^oF	degrees Fahrenheit
DBP	disinfection byproduct
E. coli	*Escherichia coliform*
flux	volume or mass of permeate passing through the membrane per unit area per unit time
fouling	deposition of material such as colloidal matter, microorganisms, and metal oxides on the membrane surface or in its pores, causing a decrease in membrane performance
g	gravitational pull
gpm	gallons per minute
hr	hour
in	inch

kWh	kilowatt-hour
log_{10}	logarithmic (base 10)
R2A	low-nutrient agar for heterotrophic bacteria assay
Metropolitan	Metropolitan Water District of Southern California
µg/L	micrograms per liter
µL	microliter
µm	micrometer
mg/L	milligrams per liter
mJ/cm^2	millijoules per square centimeter
mL	milliliter
mm	millimeter
mgd	mgdgallons per day
mW/cm^2	milliwatts per square centimeter
min	minute
normalized flux	permeate flow rate through the membrane adjusted to constant operating conditions
ND	not detected
NS	not sampled
pH	the negative log_{10} concentration of the activity of hydrogen ions
PFU/mL	plaque forming units per milliliter
PVC	polyvinyl chloride

PIER	Public interest energy research
RD&D	Research, development, and demonstration
rejection	measure of a pressure-driven membrane's ability to retard or prevent passage of solutes and other contaminants through the membrane barrier
RO	reverse osmosis - pressure-driven membrane separation process to removes ions, salts, and other dissolved solids and nonvolatile organics controlled by the diffusion rate of solutes through the membrane barrier and by sieving and typically used for desalting, specific ion removal, and natural and synthetic organics removal
scale	coating or precipitate deposited on surfaces
SDI	silt density index - empirical measure of the plugging characteristics of membrane feedwater based on passing the water through a membrane filter test apparatus containing a 0.45-micrometer pore diameter filter
sec	second
specific flux	permeate (water) flux divided by the net driving pressure
TDS	total dissolved solids - weight per unit volume of solids remaining after a sample has been filtered to remove suspended and colloidal solids
USEPA	United States Environmental Protection Agency
UV	ultraviolet
W	watt

TABLES AND FIGURES

Table 1. Analytical scheme for reverse osmosis treatment evaluation

Parameter	Sampling Method	Sampling Location		
		RO Influent	RO Permeate	RO Brine
pH	On-Line	Continuous	NA	NA
Temperature	On-Line	Continuous	NA	NA
Conductivity	Grab	1/day	1/day	1/day
Turbidity	On-Line	Continuous	NA	NA
Flow	On-Line	Continuous	Continuous	Continuous
Pressure	On-Line	Continuous	Continuous	Continuous
SDI	Grab	1/week	NA	NA
Alkalinity/Hardness	Grab	Biweekly	Biweekly	Biweekly
TDS	Grab	Biweekly	Biweekly	Biweekly
Major Cations (Ca/K/Mg/Na)	Grab	Biweekly	Biweekly	Biweekly
Major Anions ($Br/Cl/F/NO_3/SO_4$)	Grab	Biweekly	Biweekly	Biweekly
Trace Metals (Al/As/Ba/Fe/Mn/Sr)	Grab	Biweekly	Biweekly	Biweekly
Silica	Grab	Biweekly	Biweekly	Biweekly
DOC	Grab	Biweekly	Biweekly	Biweekly
UV_{254}	Grab	Biweekly	Biweekly	Biweekly
HPC Bacteria	Grab	Biweekly	Biweekly	Biweekly

NA = not applicable

Table 2. Water quality during MS-2 biodosimetry challenges

Parameter	Average ± Standard Deviation	Units
Hardness*	210 ± 3.5	mg/L as $CaCO_3$
pH*	7.9 ± 0.1	units
Turbidity (filter effluent)*	0.07 ± 0.01	NTU
UV absorbance at 254 nm*	0.01 ± 0.005	1/cm
UV Transmittance*, ‡	96.8 ± 1.0	percent

* Measured at the filter effluent (post-ozonation)
† Temperature decreased across the study period
‡ Based on UV absorbance readings

Table 3. Plant data for 185-mgd permeate capacity reverse osmosis system

Parameter	Value	
	8-in. RO System	16-in. RO System
Membrane element size	8-in. x 40-in.	16-in. x 60-in.
Membrane type	Ultra-low-pressure polyamide RO	Ultra-low-pressure polyamide RO
Membrane "effective" area/element	380 ft^2	1,950 ft^2
Number of pressure vessels/train	143	143
Number of elements/ pressure vessel	6	4
Membrane permeate capacity/train	5.0 mgd	16.8 mgd
Number of treatment trains	37	11
Train footprint	1,600 ft^2/train	2,200 ft^2/train
Membrane unit recovery	85 percent	85 percent
Plant operating factor	98 percent	98 percent
Membrane flux	15 gal/ft^2/day	15 gal/ft^2/day
Influent TDS	750 mg/L	750 mg/L
Applied feed pressure	140 psi	168 psi (140 psi*)
Permeate pressure	10 psi	10 psi
Feed water temperature	64ºF [18°C]	64°F [18°C]

*Data in parentheses is for second-generation prototype elements with improved specific flux.

Table 4. Water quality during UV reactor evaluation

Parameter	Range	Units
Alkalinity[*]	96 - 109	mg/L as $CaCO_3$
Bromate[*]	ND	mg/L
Bromide[*]	0.09 - 0.10	mg/L
Hardness[*]	200 - 223	mg/L as $CaCO_3$
Heterotrophic bacteria[*]	16,652 ± 7,526[‡]	CFU/mL
pH[*]	8.0 - 8.5	units
Temperature[*]	77.7 - 52.9[†]	^oF
Turbidity (plant influent)	0.5 - 3.0	NTU
Turbidity (filter effluent)[*]	0.03 - 0.28	NTU
	0.06 ± 0.03[‡]	NTU
UV absorbance at 254 nm[*]	0.022 - 0.043	1/cm
UV Transmittance[*, **]	90.7 - 95.2	percent

[*] Measured at the filter effluent (post-ozonation)
[†] Temperature decreased across the study period
[‡] Average ± standard deviation
[**] Based on UV absorbance readings

Table 5. Operational parameters during UV reactor evaluation

Parameter	Average ± Standard Deviation	Units
Ozone dose	1.1 ± 0.3[*]	mg/L
Virus credit by ozone	2.6 ± 1.2[*]	log_{10}
Giardia credit by ozone	1.3 ± 0.5[*]	log_{10}
Ferric Chloride dose	4.4 ± 1.3[*]	mg/L
Cationic polymer dose	0.9 ± 0.2[*]	mg/L
Filtration rate	5.1 ± 0.1	gpm/ft^2
UV process		
kilowatt-hours/1000 gallons treated	0.10 ± 0.03	kWh/1,000 gal
Increase in water temperature	0.08 ± 1.1	^oF
Flow	2.93 ± 0.04	mgd
Starts/day		
Lamp 1	1.6 ± 0.6	starts/day
Lamp 2	1.6 ± 0.7	starts/day
Lamp 3	1.3 ± 0.2	starts/day
Lamp 4	1.7 ± 0.5	starts/day

[*] Does not include periods when ozone or chemical feed was shut-down

Table 6. UV reactor sensor readings

Study Period, Unit of Measure	Sensor Reading per Lamp Number			
	1	2	3	4
First 768 hr*				
High reading	45	53	56	55
75th percentile reading	36	43	46	44
Median reading	30	42	41	39
25th percentile reading	29	39	40	37
Low reading	24	33	33	30
During loss of chemical feed				
Median reading	13	18	17	16
During loss of preoxidation				
Median reading	14	24	N/A	19
From 792 hr to end of study†				
High reading	35	53	41	39
75th percentile reading	32	48	30	38
Median reading	29	41	26	37
25th percentile reading	27	44	21	36
Low reading	17	31	19	18

* Before the loss of coagulant and polymer feed at 768 hours

† Does not include data during loss of pre-oxidation or during lamp failures

Table 7. Effect of sensor well position on sensor reading

Sensor Location	Sensor Reading			
	1	2	3	4
Initial readings (in proper wells)	70.1	98.4	75.2	81.0
Switching sensors 1 and 2*	100.8	76.9		
Switching sensors 3 and 4†			113.0	55.8
Final readings (in proper wells)	70.3	109.4	73.7	84.2

* Sensor 1 placed in well 2 (above lamp 2) and sensor 2 placed in well 1 (above lamp 1)

† Sensor 3 placed in well 4 (above lamp 4) and sensor 4 placed in well 3 (above lamp 3)

Table 8. Change in water quality and sensor readings during loss of preoxidation

Period of Change*	Percent Change in Value (percent)						
	UV Transmittance	Turbidity	Particles	Sensor 1	Sensor 2	Sensor 3	Sensor 4
A† (0 to 175 min)	N/C	N/C	9.6	-0.7	-0.7	+1.0	-0.6
B† (175 to 230 min)	-1.0	45.8	37.9	-14.9	-14.8	-15.2	-15.5
C† (230 to 275 min)	-0.2	4.3	11.5	-2.4	-2.1	-2.4	-1.8
D† (275 to 375 min)	-1.2	42.5	70.0	-16.7	-16.4	-16.6	-16.8
E† (375 to 600 min)	-0.3	N/C	-1.2	-4.5	-4.8	-3.7	-4.8
B-*E*‡ (0 to 600 min)	-2.5	116.7	158.0	-33.9	-33.7	-33.5	-34.2

N/C No net change in value
* For further explanation of when these periods occurred, see Figure 14
† Change calculated from beginning to end of individual period
‡ Change calculated from beginning of period B to end of study (cumulative change), so individual changes may not equal cumulative change

Table 9. Operational data of reverse osmosis pilot unit

	Reverse Osmosis Element Size	
Parameter	8-Inch	16-Inch
Feed pressure (psi)	79.5	99.4
Differential pressure (psi)	8.6	7.2
Operating flux (gfd)	14.8	14.2
Process recovery (percent)	14.1	13.6
Specific flux (gfd/psi)[†]	0.28	0.21
Normalized operating pressure (psi)[‡]	66.0	82.3
Salinity rejection (percent)	98.7	98.4
Energy usage (kWh/1,000 gal)[§]	0.60	0.75
Cleaning frequency (months)	1 to 2	1 to 2

[†] Normalized to 25ºC
[‡] Assume flux = 15 gfd, temperature = 25ºC
[§] Pump efficiency = 80 percent

Table 10. Water quality data for reverse osmosis study

Parameter	Reverse Osmosis Element Size	
	8-Inch Rejection (percent)	16-Inch Rejection (percent)
Inorganics		
Alkalinity	96.9 (5, 0.5)*	97.2 (5, 0.2)
Total hardness	99.6 (5, 0.2)	99.5 (5, 0.0)
Total dissolved solids	98.7 (5, 0.8)	98.4 (5, 0.6)
UV absorbance at 254 nm	94.3 (5, 3.8)	93.9 (5, 3.4)
Calcium	99.7 (3, 0.2)	94.5 (3, 8.7)
Magnesium	99.8 (3, 0.0)	99.3 (3, 0.7)
Potassium	95.5 (3, 2.0)	96.7 (3, 2.5)
Sodium	97.6 (3, 0.2)	97.4 (3, 0.1)
Nitrate	93.5 (4, 1.2)	93.5 (4, 0.4)
Silica	97.6 (5, 1.0)	94.4 (5, 7.3)
Chloride	97.9 (5, 0.6)	98.2 (5, 0.7)
Sulfate	98.2 (5, 0.4)	98.3 (5, 0.5)
Fluoride	95.5 (5, 0.0)	95.4 (5, 0.0)
Trace Metals		
Barium	97.1 (5, 1.8)	98.3 (5, 1.9)
Aluminum	66.5 (5, 36.9)	67.6 (3, 22.4)
Iron	28.7 (5, 33.4)	35.4 (4, 40.8)
Strontium	99.2 (5, 0.9)	99.3 (5, 0.8)

*Data in parenthesis indicate number of samples and standard deviation, respectively.

Table 11. Capital cost assumptions for reverse osmosis

Item	8-in. RO System	16-in. RO system
Membranes		
Membrane	$600/element	$2,950/element
Installation	$50/element	$400/element
Pressure vessels		
Vessel	$1,400/vessel	$4,500/vessel
Installation	$140/vessel	$450/vessel
Skid piping	$300,000/train	$200,000/train
Support frame	$94,500/train	$62,500/train
Train instruments	$25,000/train	$25,000/train
Membrane feed pumps	$150,000/each	$300,000/each
Buildings		
Membrane train area	$100/ft^2	$100/ft^2
Other areas	$120/ft^2	$120/ft^2
Site development	$25,000/acre	$25,000/acre
Electrical	10 percent of equipment cost	10 percent of equipment cost
Plant controls	10 percent of equipment cost	10 percent of equipment cost
Construction contingency	25 percent of capital costs	25 percent of capital costs
Overall project contingency	20 percent of capital costs (including construction contingency)	20 percent of capital costs (including construction contingency)
Interest rate	6 percent	6 percent
Amortization period	20 years	20 years

Table 12. Operation and maintenance cost assumptions for reverse osmosis

Item	8-in. RO System	16-in. RO system
Labor		
Number of operators	30	30
Operator salary	$40,000/yr	$40,000/yr
Overhead	40 percent of labor	40 percent of labor
Chemicals		
Acid (93% H_2SO_4)	$0.04/lb	$0.04/lb
Scale inhibitor	$1.04/lb	$1.04/lb
Caustic (50% NaOH)	$0.14/lb	$0.14/lb
Cleaning chemicals	$0.015/kgal of permeate	$0.015/kgal of permeate
Cartridge filters	$5.40/cartridge	$5.40/cartridge
Other materials	$0.03/kgal	$0.03/kgal
Power	$0.06/kWh	$0.06/kWh
Pump efficiency	76 percent	76 percent
Motor efficiency	92 percent	92 percent
Plant operating factor	98 percent	98 percent
Membrane life	5 years	5 years
Membrane replacement	$600/element	$2,950/element

Table 13. Breakdown of capital costs for 8-inch and 16-inch reverse osmosis system

Parameter	Cost ($M)		
	8-inch RO System	16-Inch RO System	Percent Difference
Membrane cost	20.6	21.3	+3.4
Pressure vessels	8.15	7.79	-4.4
Skid piping	11.1	2.20	-80
Support frame	3.50	0.69	-80
Membrane feed pumps	8.39	5.00	-40
Other installed membrane train equipment	17.8	13.1	-26
Additional process items	11.3	11.3	0
Buildings	14.7	11.2	-24
Site development	0.63	0.63	0.0
Electrical	6.96	5.01	-28
Plant controls	6.96	5.01	-28
Other facilities	3.5	3.5	0
Construction contingency	28.4	21.7	-24
Overall project contingency	28.6	21.8	-24
Total capital	170.59	130.23	-24

Table 14. Total cost for a 185-mgd reverse osmosis system

Cost Component	Reverse Osmosis Element Size 8-in.	16-in.
Energy ($M/year)	7.41	8.89 (7.41*)
Labor ($M/year)	1.68	1.68
Chemicals ($M/year)	3.98	3.98
Membrane replacement ($M/year)	3.81	3.75
Miscellaneous ($M/year)	2.52	2.48
Annual O&M ($M/year)	**19.4**	**20.8 (19.3*)**
Total Capital RO Cost ($M)	**170.6**	**130.2**
Annual RO Capital Cost ($M/year)	**14.9**	**11.4**
Total Annual RO System Cost ($M/year)	**34.3**	**32.2 (30.7*)**

* Data in parentheses assumes second-generation prototype elements with improved specific flux.

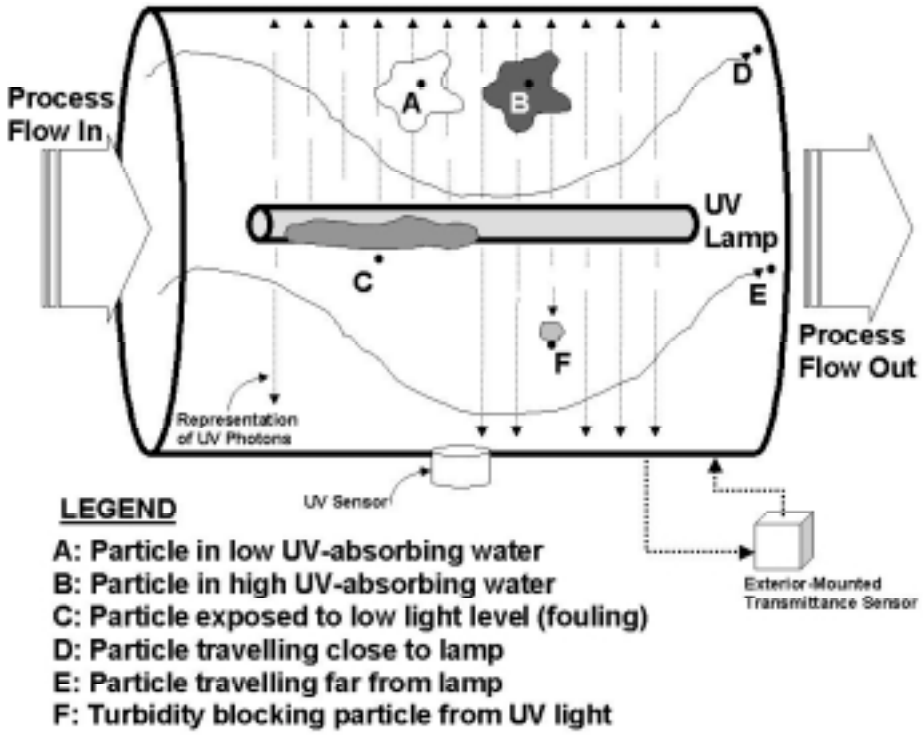

Figure 1. Water quality and process variables affecting transferred UV dose

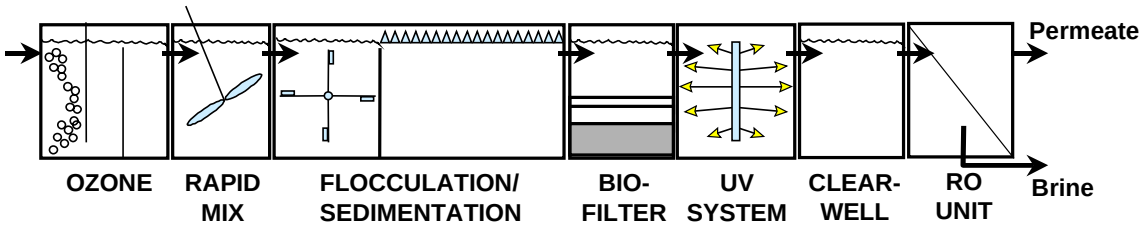

Figure 2. Conventional treatment plant processes integrated with ozone and UV

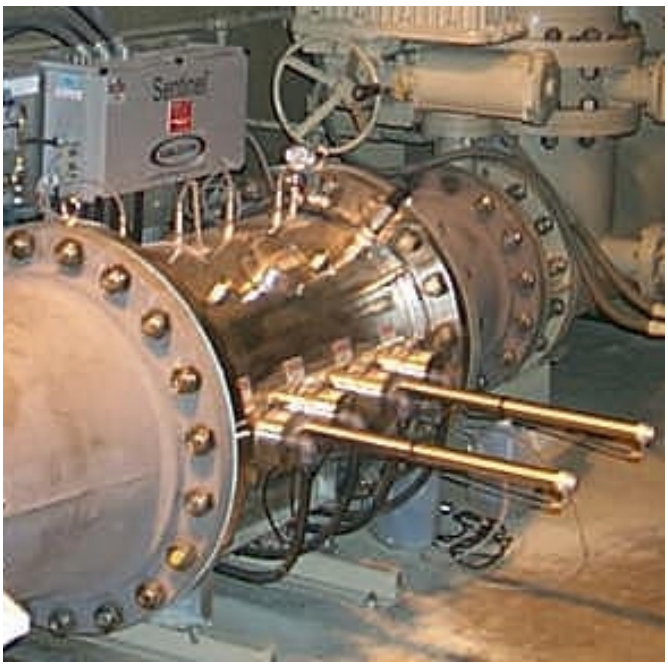

Figure 3. Medium-pressure UV reactor treating filtered water

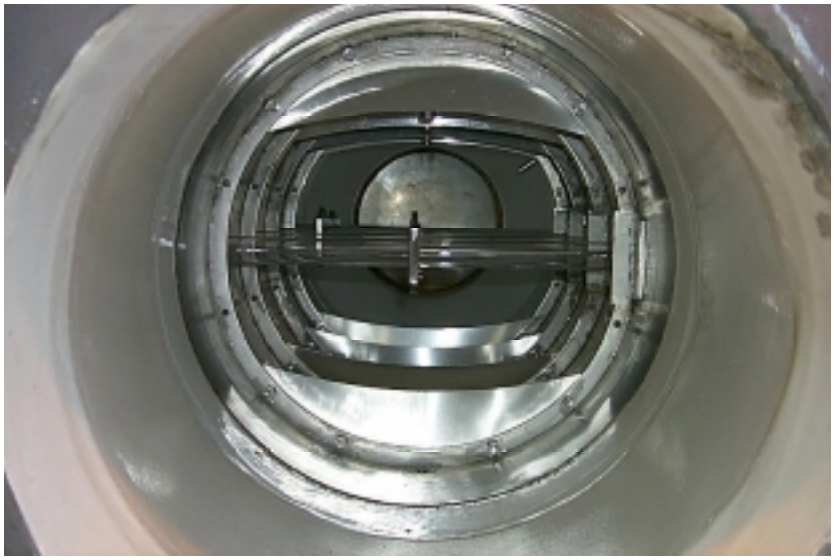

Figure 4. Interior view of the UV reactor showing ring- and crescent baffles around the pipe circumference

Figure 5. Sensor wells mounted at the top of the UV reactor

Figure 6. Stainless-steel brush wiper mechanism for UV lamp quartz sleeves

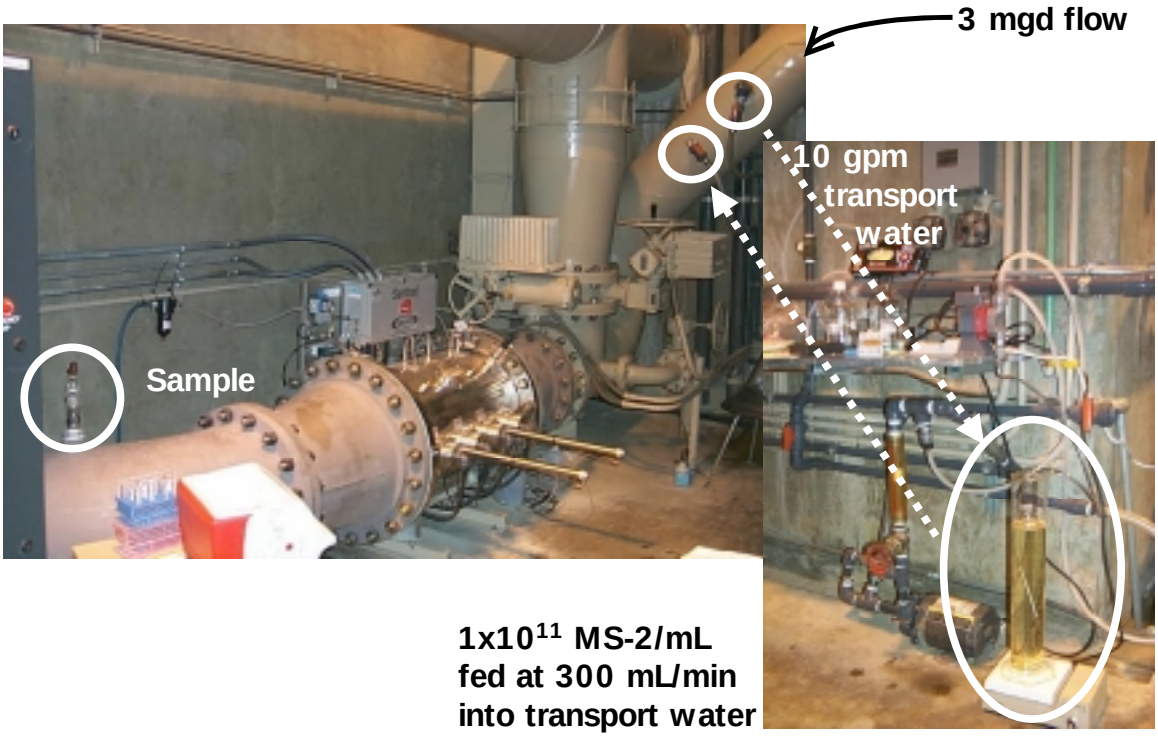

Figure 7. Biodosimetry challenge setup showing injection and sample ports for MS-2

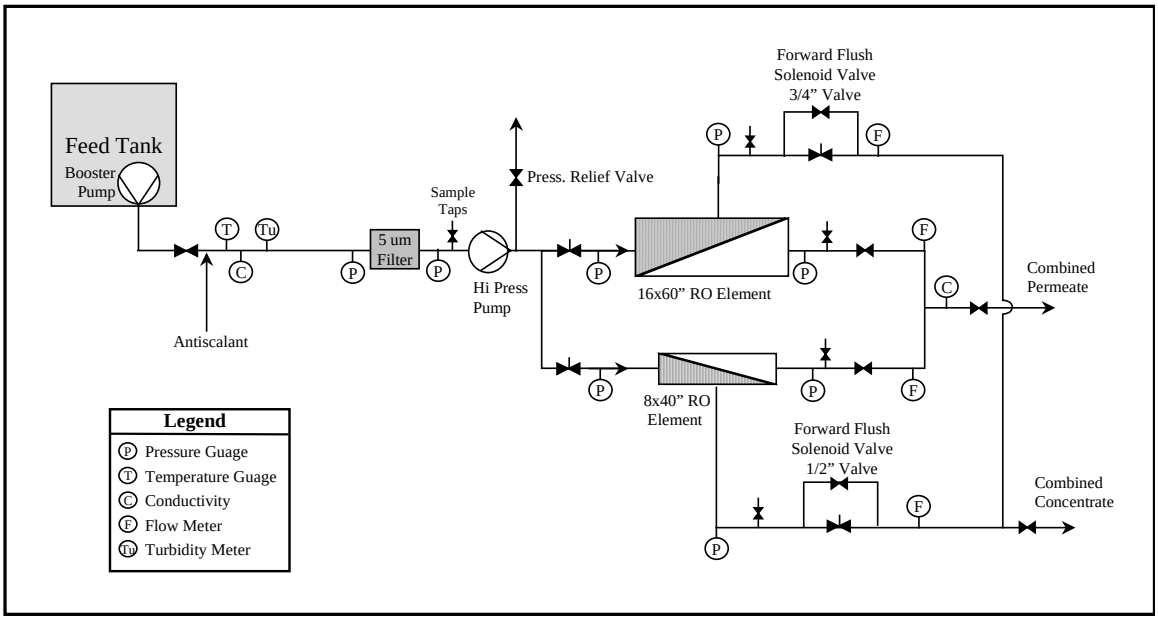

Figure 8. Schematic diagram of reverse osmosis unit

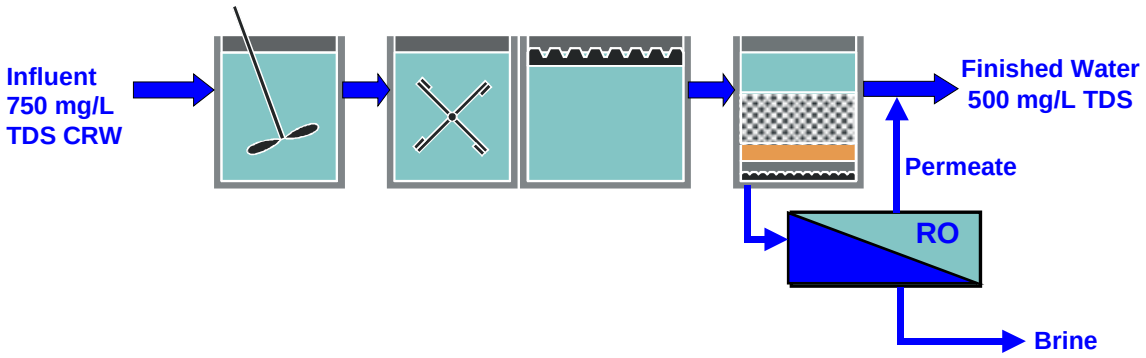

Figure 9. Conceptual diagram of a split-flow desalting facility

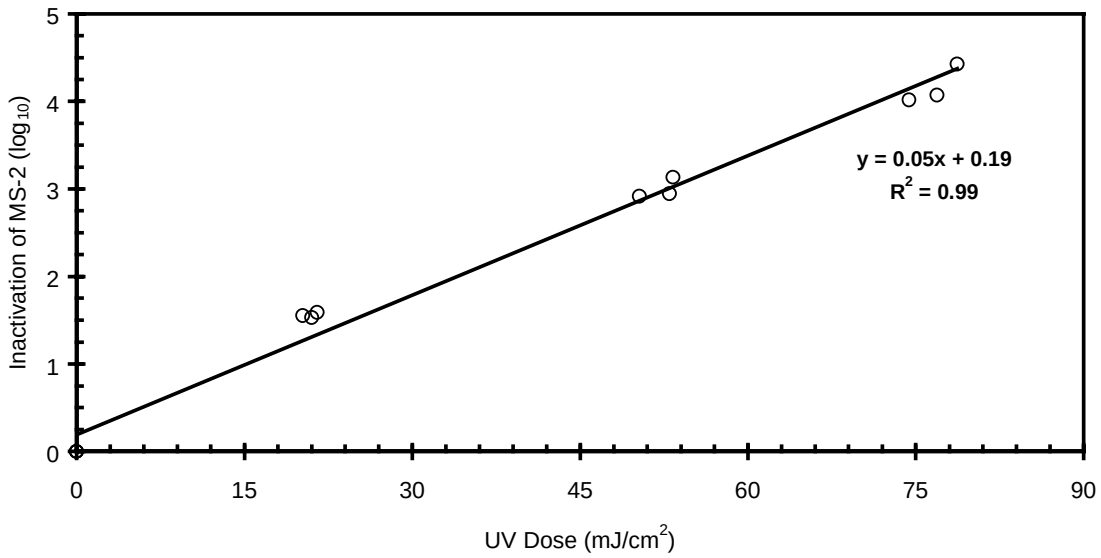

Figure 10. Collimated beam inactivation of MS-2 (low-pressure UV lamp)

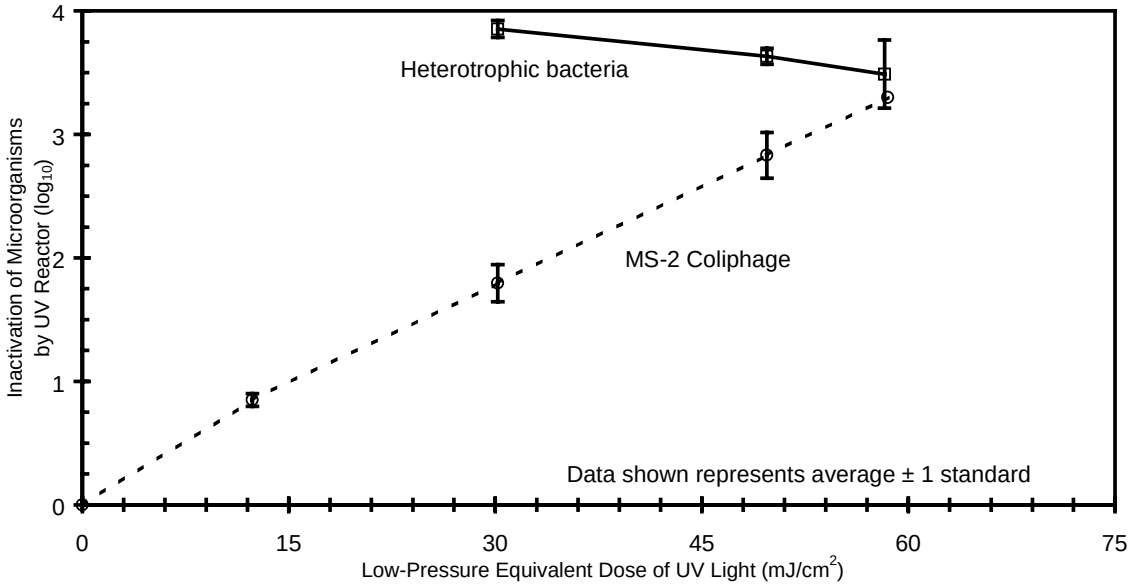

Figure 11. Inactivation of microorganisms with UV reactor, plotted against low-pressure equivalent UV dose

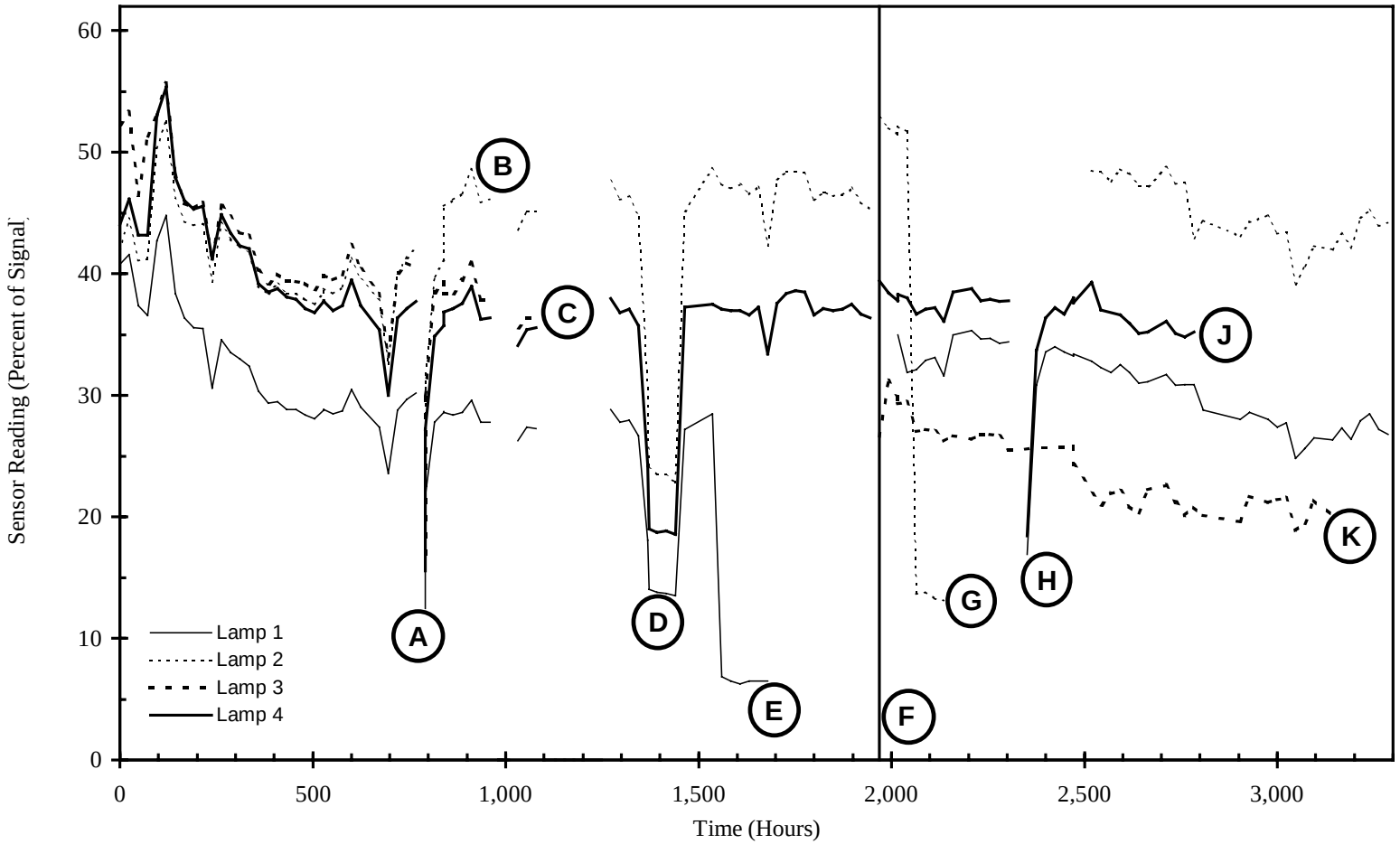

Figure 12. UV sensor performance across the test period

Legend							
A	Loss of coagulant/polymer feed	D	Loss of pre-oxidant	G	Lamp 2 failure	K	Lamp 3 failure
B	Reactor off-line	E	Lamp 1 failure	H	Change in source water		
C	Reactor off-line, lamp 3 failure	F	Replacement of all 4 lamps	J	Lamp 4 failure		

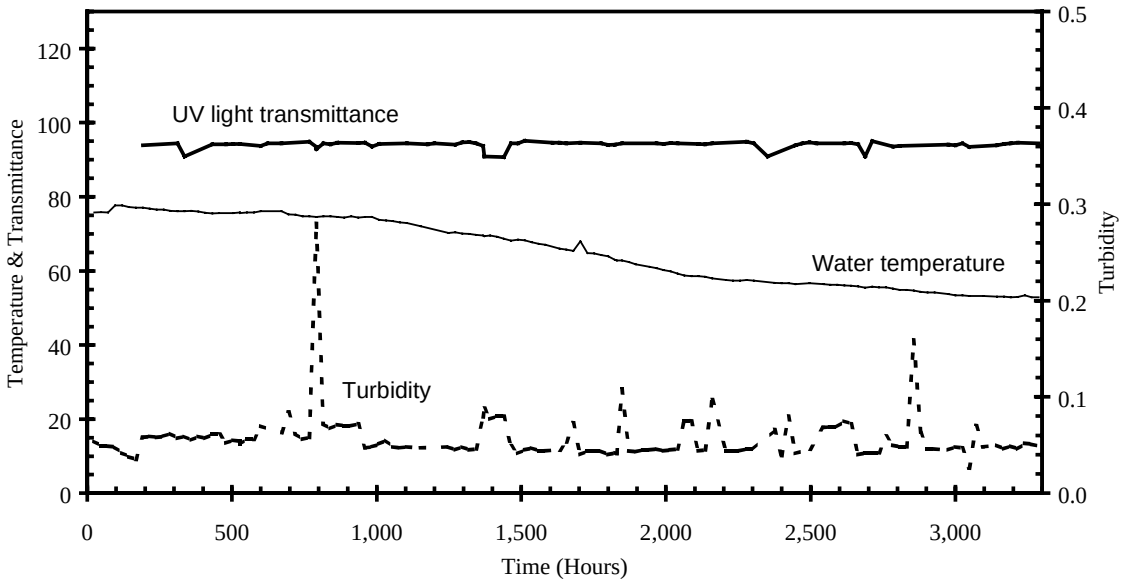

Figure 13. Transmittance, temperature, and turbidity fluctuation during the study period for the UV reactor

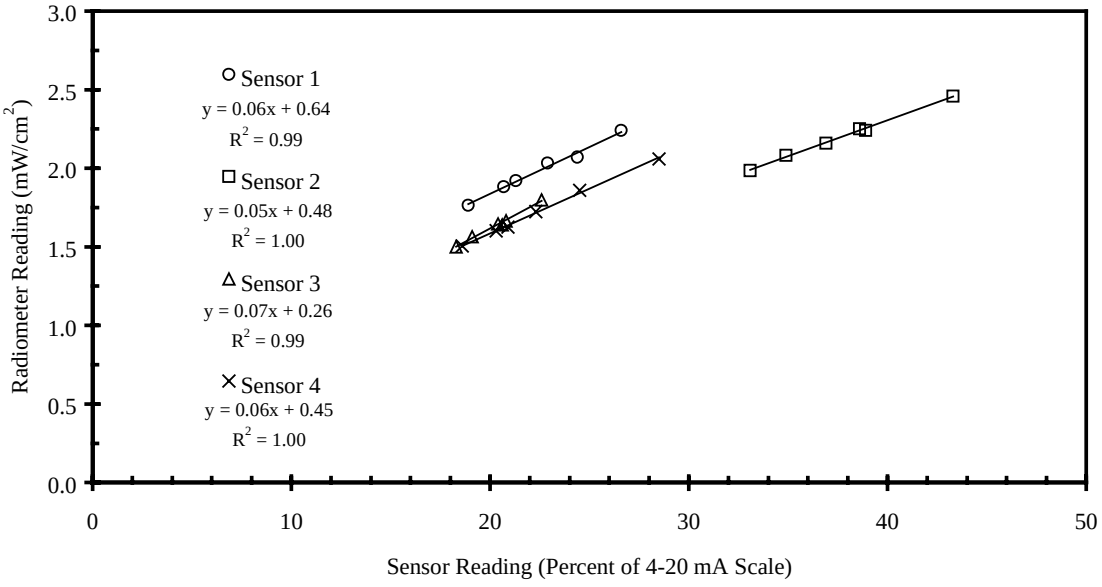

Figure 14. Relationship between UV sensor and calibrated radiometer

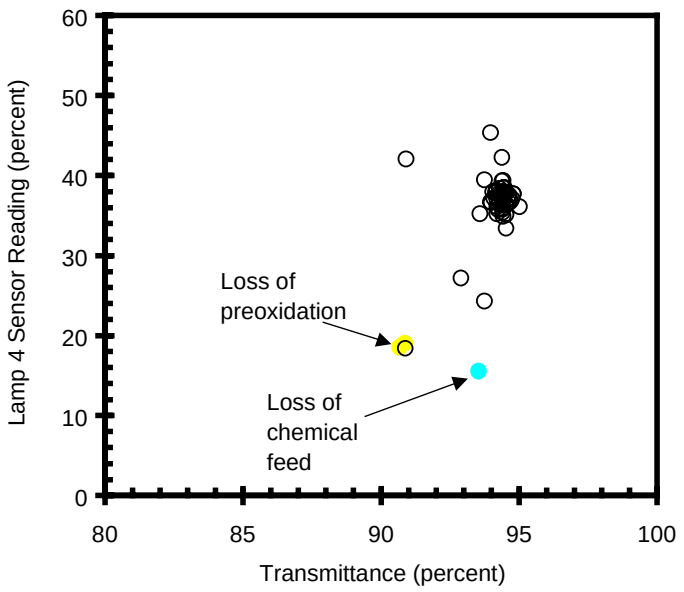

(a) Effects of changes in water transmittance

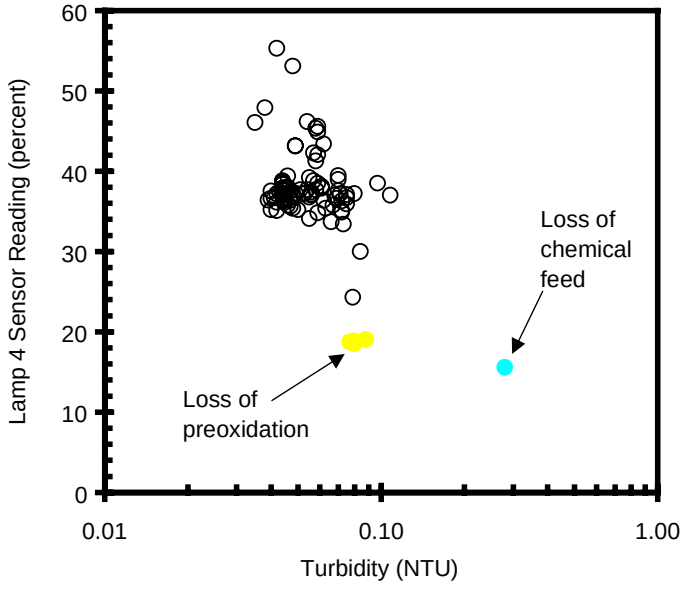

(b) Effects of changes in water turbidity

Figure 15. Effect of water quality on UV sensor performance (filled data points represent data collected during process upsets)

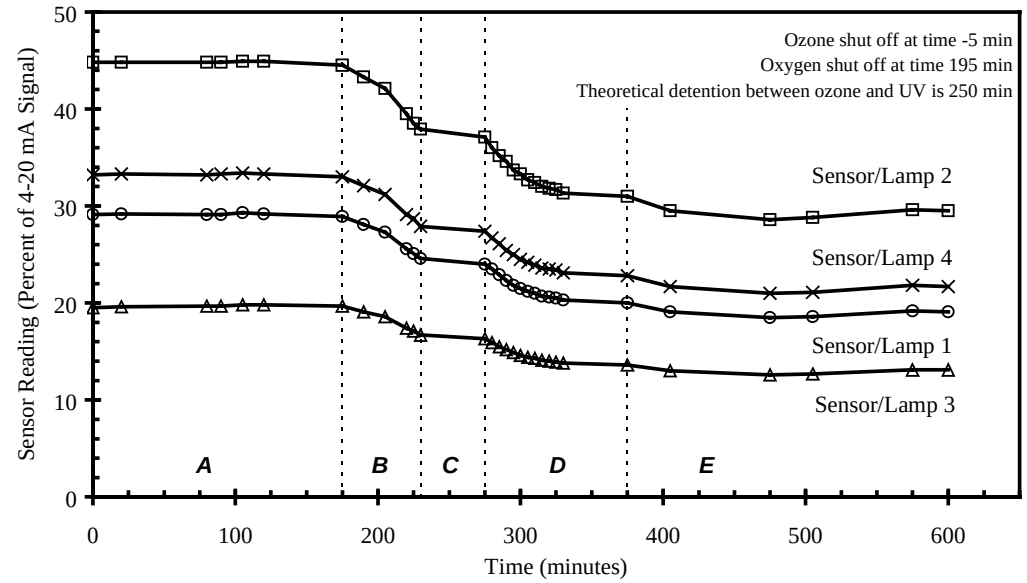

(a) Sensor performance

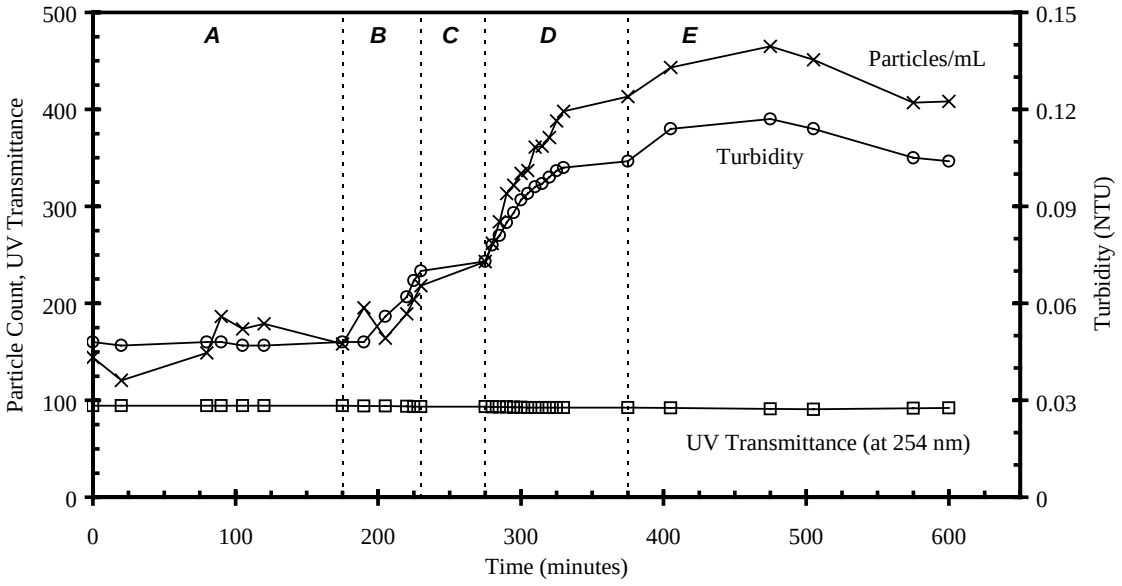

(b) Filter effluent water quality

Figure 16. Effect of loss of preoxidation on sensor performance

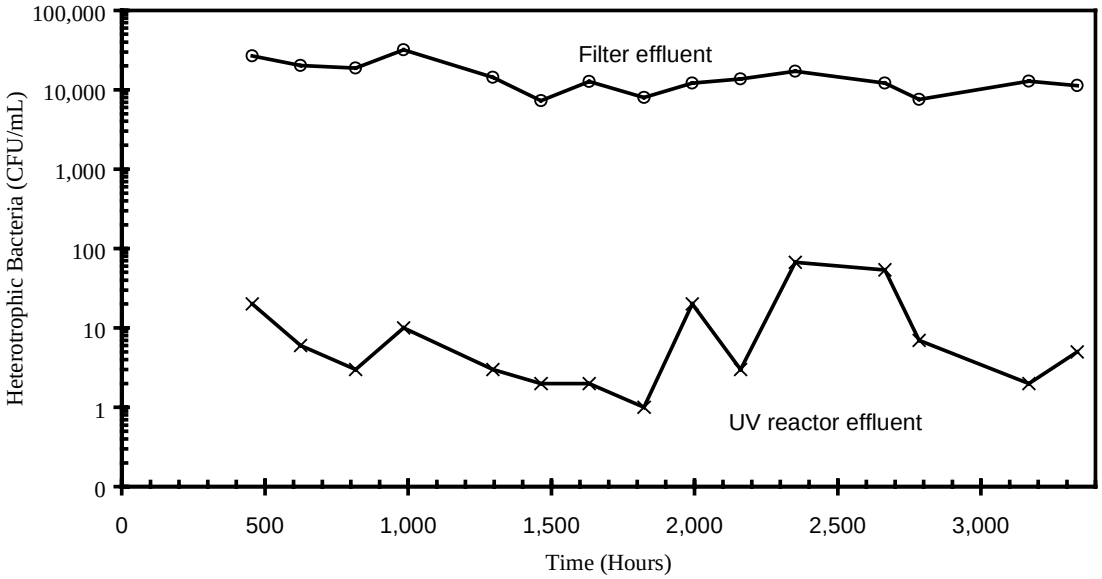

Figure 17. Effect of UV treatment on the level of heterotrophic bacteria in water

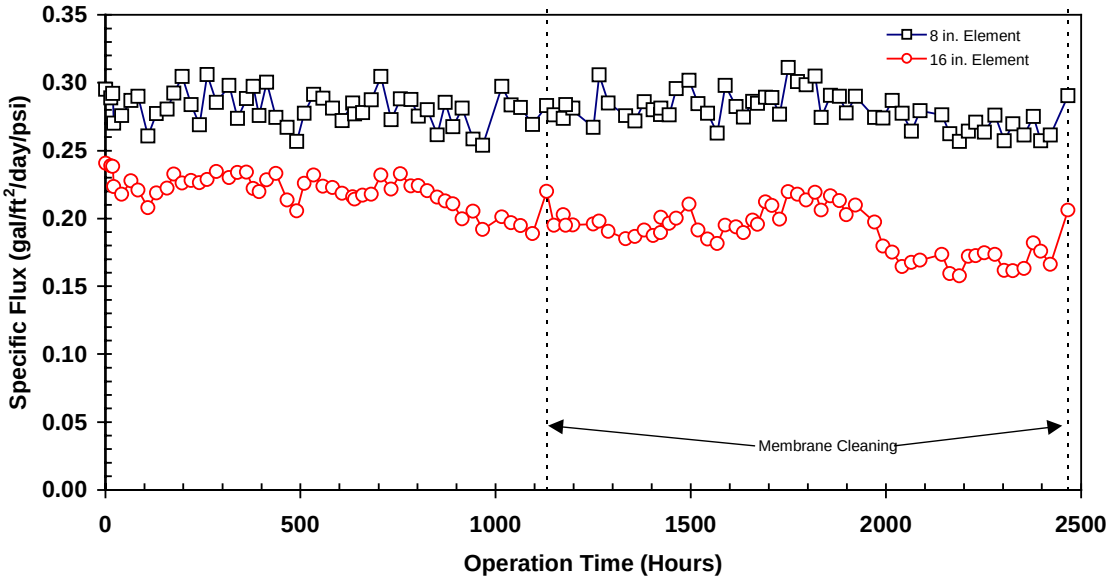

Figure 18. Specific flux for pilot-scale test unit

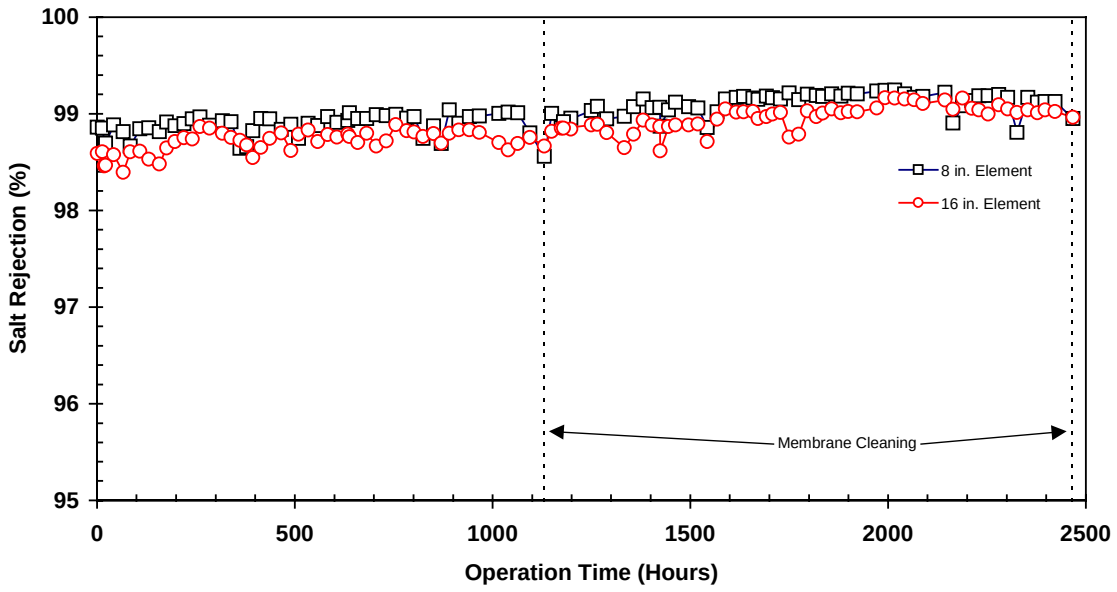

Figure 19. Salt rejection for pilot-scale test unit

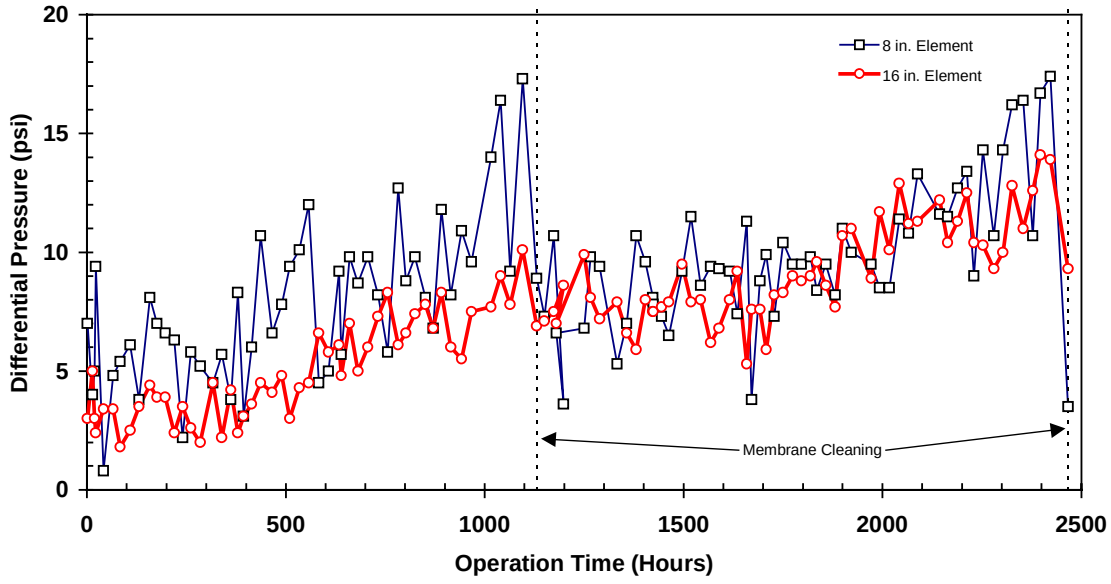

Figure 20. Differential pressure across the element for pilot-scale test unit

APPENDICES

Appendix A

Water Quality Methods

All water quality sampling was conducted by Metropolitan's staff. Inorganic and microbial analyses were analyzed at Metropolitan's Water Quality Laboratory in La Verne, Calif. The water quality constituents were analyzed according to the methods described below. *Standard Methods for the Examination of Water and Wastewater* (APHA 1998) was referenced for sample analysis wherever possible.

Inorganic Constituents

Alkalinity and Hardness were analyzed by titration according to Standard Methods 2320B and 2340C (APHA 1998).

Total Dissolved Solids (TDS) was measured using Standard Method 2540C (APHA 1998) or estimated from conductivity measurements.

Bromate, Bromide, Chloride, Fluoride, Nitrate, and Sulfate were analyzed using a modified EPA Method 300.0 and a Dionex Model DX300 ion chromatograph. The minimum reporting levels (MRL) for each constituent (in mg/L) are: BrO_3^-: 0.003, Br: 0.02, Cl: 2.0, F: 0.02, NO_3: 0.05, and SO_4: 4.0.

Silica levels were determined according to Standard Method 4500-Si D (APHA 1998) using a Shimadzu UV-2401PC ultraviolet/visible spectrophotometer.

Boron was measured using the Curcumin method as absorbance at 540 nm on a spectrophotometer against a standard curve using Standard Method 4500-B (APHA 1998).

Calcium, Magnesium, Potassium, Sodium were analyzed according to Standard Method 3111B (APHA 1998) using a Varian SpectrAA-300/400 atomic absorption spectrophotometer. The MRL for this method is 0.1 mg/L for each constituent.

Aluminum, Arsenic, Iron, Manganese, Barium and Strontium (trace metals) were analyzed according to EPA Method 200.8 using a Perkin Elmer Elan 6000 ICP-MS. MRLs for this method are as follows: Al: 5 μg/L, As: 0.5 μg/L, Fe: 20 μg/L; Mn: 5 μg/L; Ba: 5 μg/L, and Sr: 20 μg/L.

Total Organic Carbon (TOC) samples were analyzed by the ultraviolet/persulfate oxidation method (Standard Method 5310C, APHA 1998) using a Sievers 800 organic carbon analyzer. The MRL for this method is 0.05 mg/L.

Dissolved Organic Carbon (DOC) was defined by a filtration step involving a pre-washed 0.45 micron nylon membrane filter. DOC samples are analyzed by the ultraviolet/persulfate oxidation method (Standard Method 5310C, APHA 1998) using a Sievers 800 organic carbon analyzer. The MRL for this method is 0.05 mg/L.

Ultraviolet Light Absorbance and Transmittance samples were analyzed at 254 nm using a Shimadzu UV-2401PC ultra-violet/visible spectrophotometer according to Standard Method 5910 (APHA 1995). Samples (for the reverse osmosis study) were filtered through a prewashed 0.45-μm Teflon membrane to remove turbidity which can interfere with UV measurement. Samples collected for the UV reactor study were not filtered. UV transmittance was calculated based on absorbance readings, and used the Beer-Lambert law.

Free and Total Chlorine was measured using Standard Method 4500-Cl G (APHA 1998). For all free chlorine samples, 200 μl of 0.03 *N* thioacetamide solution per 10 mL of sample was added to control for interference by monochloramine.

Microbacteriological Constituents

Heterotrophic Plate Count (HPC) bacteria were identified and enumerated using the R2A membrane filtration technique (plating in triplicate). R2A plates are incubated at 28ºC for 7 days, according to *Standard Methods* (APHA 1998).

MS-2 coliphage was obtained from American Type Culture Collection (ATCC strain 15597-B1; ATCC, Rockville, MD), with *Escherichia coli* Famp (ATCC strain 15597) as the bacterial host. The assay was conducted according to the procedure described in the Information Collection Rule **(USEPA 1996a, USEPA 1996b)**, along with an added purification stage, and is recommended by the USEPA for simulating the inactivation of enteric viruses **(USEPA 1982)**. MS-2 was grown onto tryptone agar plates, and resuspended into a saline-calcium buffer solution. MS-2 stock solution was purified by centrifugation (15 minutes at 10,000x*g* and 4 °C) followed by membrane filtration (0.22 μm porosity). The added purification, conducted prior to each experiment, further purified an aliquot of MS-2 stock solution with spin columns (TE Super Select-D, G-50; 5'→3', Inc., Boulder, Colorado) to remove any contaminants that may interfere with UV irradiation. The resulting titer was diluted to approximately $1x10^8$ plaque forming units per milliliter (PFU/mL).

The MS-2 host (*E. coli* Famp) was incubated in tryptone broth overnight at 37 °C, then transferred into new tryptone broth and incubated for 4 hours at 37 °C to allow maximum pili expression. Propagation was performed using a double-agar overlay procedure **(Adams 1959)** described by **Wolfe et al. (1989)**. One mL of the *E. coli* 4-hour culture was added to test tubes containing warm (45 °C) tryptone agar, immediately followed by the addition of 1 mL of MS-2 sample for appropriate dilution. The test tube was rapidly rolled between the palms of the analyst's hands and dispensed over a tryptone agar petri plate. Plates were incubated for 20 hours at 37 °C. Samples were run in triplicate.

MS-2 positive controls consisted of MS-2 coliphage stock solution before and after spin column purification. Negative controls consisted of sterile saline-calcium solution (experiment

negative control), *E. coli* not infected with MS-2, and sterile media to account for agar contamination in the incubator.

Total Coliforms and *E. Coli.* were identified and enumerated according to *Standard Methods* (APHA 1998). Pretreatment influent and RO concentrate samples were analyzed using multiple tube fermentation methods and pretreatment effluent and RO permeate streams were analyzed using the membrane filtration option per *Standard Methods*.

Appendix B

Supporting Calculations

In order to assess the performance of the pretreatment and salinity reduction steps, several key values were calculated based on raw process data. These calculated values include silt density index (SDI) for the pretreatment step and specific normalized flux, salt passage, and energy consumption for the RO system. These values were calculated using the following methods:

Specific Ultra Violet Light Absorbance at 254 nm (SUVA) was calculated by dividing the measured UV light absorbance at 254 nm (m^{-1}) by the measured TOC (mg/L) and multiplying by 100.

Silt Density Index (SDI) was measured using the method described by the American Society for Testing and Materials (ASTM) method D4189-82. The initial time (t_o) and the time after 15 minutes of continuous flow (t_{15}) to collect 500 ml through a 0.45 μm Millipore filter (Type HA, Millipore Corp., Bedford, Mass.) at 30 psig were measured. SDI was calculated using the following equation:

$$SDI = \left[\frac{1 - \frac{t_o}{t_{15}}}{15} \right] * 100$$

where t_o = initial time in seconds to collect 500 ml

t_{15} = time in seconds to collect 500 ml after 15 minutes

Specific flux was calculated by the following equations:

$$\text{Specific Flux} = (T_{Corr} * Q_{Permeate})/(a * P_{net}) \qquad [gal/ft^2/day/psi]$$

where T_{Corr} = Feed Temperature correction factor

$$T_{Corr} = e^{(U* ((1/T) - (1/298))}$$

where U = 3100 for Koch Fluid Systems ULP-TFC membranes

T = Measured temperature [°C]

$Q_{Permeate}$ = Permeate flow [gal/day]

a = Membrane surface area [ft^2]

$$P_{Net} = P_{Feed} - \Delta\pi - \Delta P_{Hydraulic} - P_{Permeate} \quad [psi]$$

where $\Delta\pi$ = Differential osmotic pressure [psi]

$$\Delta\pi = 0.01 * (\Omega_{Average} - \Omega_{Permeate}) * (K_{Feed} + K_{Brine})/2$$

where K = Conversion factor from conductivity to TDS

[(mg/L)/(µS/cm)]

Ω = Conductivity [µS/cm]

Salt rejection was calculated by the following equation:

Salt rejection = [1-(permeate TDS/feed TDS)] x 100